

World Journal of *Clinical Cases*

World J Clin Cases 2023 January 26; 11(3): 487-718



MINIREVIEWS

- 487 Protective effects of combined treatment with ciprofol and mild therapeutic hypothermia during cerebral ischemia-reperfusion injury
Wang YC, Wu MJ, Zhou SL, Li ZH
- 493 Non-pulmonary involvement in COVID-19: A systemic disease rather than a pure respiratory infection
El-Kassas M, Alborai M, Elbadry M, El Sheemy R, Abdellah M, Afify S, Madkour A, Zaghloul M, Awad A, Wifi MN, Al Balakosy A, Eltabbakh M
- 506 Progress and expectation of stem cell therapy for diabetic wound healing
Xu ZH, Ma MH, Li YQ, Li LL, Liu GH
- 514 Prevention, diagnostic evaluation, management and prognostic implications of liver disease in critically ill patients with COVID-19
Valsamaki A, Xanthoudaki M, Oikonomou KG, Vlachostergios PJ, Papadogoulas A, Katsiafylloudis P, Voulgaridi I, Skoura AL, Komnos A, Papamichalis P
- 528 Exosomal miRNA in early-stage hepatocellular carcinoma
Wu ZQ, Zhu YX, Jin Y, Zhan YC
- 534 Impact of multidrug resistance on the management of bacterial infections in cirrhosis
Terra C, de Mattos ÁZ, Chagas MS, Torres A, Wiltgen D, Souza BM, Perez RM
- 545 Could there be an interplay between periodontal changes and pancreatic malignancies?
Ungureanu BS, Gheorghe DN, Nicolae FM, Râmboiu S, Radu PA, Șurlin VM, Strâmbu VDE, Gheonea DI, Roman A, Șurlin P

ORIGINAL ARTICLE**Retrospective Study**

- 556 Qixue Shuangbu decoction and acupuncture combined with Western medicine in acute severe stroke patients
Gou LK, Li C
- 566 Successful treatment of patients with refractory idiopathic membranous nephropathy with low-dose Rituximab: A single-center experience
Wang YW, Wang XH, Wang HX, Yu RH
- 576 Bowel inflammatory presentations on computed tomography in adult patients with severe aplastic anemia during flared inflammatory episodes
Zhao XC, Xue CJ, Song H, Gao BH, Han FS, Xiao SX

- 598 Clinical outcomes of AngioJet pharmacomechanical thrombectomy *versus* catheter-directed thrombolysis for the treatment of filter-related caval thrombosis

Li JY, Liu JL, Tian X, Jia W, Jiang P, Cheng ZY, Zhang YX, Liu X, Zhou M

Clinical Trials Study

- 610 Efficacy and safety of propofol target-controlled infusion combined with butorphanol for sedated colonoscopy

Guo F, Sun DF, Feng Y, Yang L, Li JL, Sun ZL

Observational Study

- 621 Application of a hospital–community–family trinity rehabilitation nursing model combined with motor imagery therapy in patients with cerebral infarction

Li WW, Li M, Guo XJ, Liu FD

CASE REPORT

- 629 Congenital biliary atresia caused by *GPC1* gene mutation in Chinese siblings: A case report

Kong YM, Yuan K, Wang CL

- 635 Rescuing “hopeless” avulsed teeth using autologous platelet-rich fibrin following delayed reimplantation: Two case reports

Yang Y, Liu YL, Jia LN, Wang JJ, Zhang M

- 645 Acute diffuse peritonitis secondary to a seminal vesicle abscess: A case report

Li K, Liu NB, Liu JX, Chen QN, Shi BM

- 655 Young thoracic vertebra diffuse idiopathic skeletal hyperostosis with Scheuermann disease: A case report

Liu WZ, Chang ZQ, Bao ZM

- 662 Relapsed primary extraskeletal osteosarcoma of liver: A case report and review of literature

Di QY, Long XD, Ning J, Chen ZH, Mao ZQ

- 669 Heterotopic pregnancy after assisted reproductive techniques with favorable outcome of the intrauterine pregnancy: A case report

Wang YN, Zheng LW, Fu LL, Xu Y, Zhang XY

- 677 Periprosthetic knee joint infection caused by *Brucella melitensis* which was first -osteoarticular brucellosis or osteoarthritis: A case report

Stumpner T, Kuhn R, Hochreiter J, Ortmaier R

- 684 Recurrent intramuscular lipoma at extensor pollicis brevis: A case report

Byeon JY, Hwang YS, Lee JH, Choi HJ

- 692 Imaging features of retinal hemangioblastoma: A case report

Tang X, Ji HM, Li WW, Ding ZX, Ye SL

- 700** Clinical and genetic diagnosis of autosomal dominant osteopetrosis type II in a Chinese family: A case report
Gong HP, Ren Y, Zha PP, Zhang WY, Zhang J, Zhang ZW, Wang C
- 709** Soft tissue tuberculosis detected by next-generation sequencing: A case report and review of literature
He YG, Huang YH, Yi XL, Qian KL, Wang Y, Cheng H, Hu J, Liu Y

ABOUT COVER

Editorial Board Member of *World Journal of Clinical Cases*, Baharudin Abdullah, MMed, Professor, Surgeon, Department of Otorhinolaryngology-Head and Neck Surgery, School of Medical Sciences, Universiti Sains Malaysia, Kubang Kerian 16150, Kelantan, Malaysia. profbaha@gmail.com

AIMS AND SCOPE

The primary aim of *World Journal of Clinical Cases* (*WJCC*, *World J Clin Cases*) is to provide scholars and readers from various fields of clinical medicine with a platform to publish high-quality clinical research articles and communicate their research findings online.

WJCC mainly publishes articles reporting research results and findings obtained in the field of clinical medicine and covering a wide range of topics, including case control studies, retrospective cohort studies, retrospective studies, clinical trials studies, observational studies, prospective studies, randomized controlled trials, randomized clinical trials, systematic reviews, meta-analysis, and case reports.

INDEXING/ABSTRACTING

The *WJCC* is now abstracted and indexed in Science Citation Index Expanded (SCIE, also known as SciSearch®), Journal Citation Reports/Science Edition, Current Contents®/Clinical Medicine, PubMed, PubMed Central, Scopus, Reference Citation Analysis, China National Knowledge Infrastructure, China Science and Technology Journal Database, and Superstar Journals Database. The 2022 Edition of Journal Citation Reports® cites the 2021 impact factor (IF) for *WJCC* as 1.534; IF without journal self cites: 1.491; 5-year IF: 1.599; Journal Citation Indicator: 0.28; Ranking: 135 among 172 journals in medicine, general and internal; and Quartile category: Q4. The *WJCC*'s CiteScore for 2021 is 1.2 and Scopus CiteScore rank 2021: General Medicine is 443/826.

RESPONSIBLE EDITORS FOR THIS ISSUE

Production Editor: *Ying-Yi Yuan*; Production Department Director: *Xiang Li*; Editorial Office Director: *Jin-Lei Wang*.

NAME OF JOURNAL

World Journal of Clinical Cases

ISSN

ISSN 2307-8960 (online)

LAUNCH DATE

April 16, 2013

FREQUENCY

Thrice Monthly

EDITORS-IN-CHIEF

Bao-Gan Peng, Jerzy Tadeusz Chudek, George Kontogeorgos, Maurizio Serati, Ja Hyeon Ku

EDITORIAL BOARD MEMBERS

<https://www.wjgnet.com/2307-8960/editorialboard.htm>

PUBLICATION DATE

January 26, 2023

COPYRIGHT

© 2023 Baishideng Publishing Group Inc

INSTRUCTIONS TO AUTHORS

<https://www.wjgnet.com/bpg/gerinfo/204>

GUIDELINES FOR ETHICS DOCUMENTS

<https://www.wjgnet.com/bpg/GerInfo/287>

GUIDELINES FOR NON-NATIVE SPEAKERS OF ENGLISH

<https://www.wjgnet.com/bpg/gerinfo/240>

PUBLICATION ETHICS

<https://www.wjgnet.com/bpg/GerInfo/288>

PUBLICATION MISCONDUCT

<https://www.wjgnet.com/bpg/gerinfo/208>

ARTICLE PROCESSING CHARGE

<https://www.wjgnet.com/bpg/gerinfo/242>

STEPS FOR SUBMITTING MANUSCRIPTS

<https://www.wjgnet.com/bpg/GerInfo/239>

ONLINE SUBMISSION

<https://www.f6publishing.com>

Retrospective Study

Bowel inflammatory presentations on computed tomography in adult patients with severe aplastic anemia during flared inflammatory episodes

Xi-Chen Zhao, Cheng-Jiang Xue, Hui Song, Bin-Han Gao, Fu-Shen Han, Shu-Xin Xiao

Specialty type: Hematology**Provenance and peer review:**

Unsolicited article; Externally peer reviewed.

Peer-review model: Single blind**Peer-review report's scientific quality classification**

Grade A (Excellent): 0

Grade B (Very good): B

Grade C (Good): C

Grade D (Fair): D

Grade E (Poor): 0

P-Reviewer: Ishfaq A, United States; Patel GR, India**Received:** October 19, 2022**Peer-review started:** October 19, 2022**First decision:** November 25, 2022**Revised:** December 3, 2022**Accepted:** January 5, 2023**Article in press:** January 5, 2023**Published online:** January 26, 2023**Xi-Chen Zhao**, Department of Hematology, The Central Hospital of Qingdao West Coast New Area, Qingdao 266555, Shandong Province, China**Cheng-Jiang Xue**, Department of Neurosurgery, The Central Hospital of Qingdao West Coast New Area, Qingdao 266555, Shandong Province, China**Hui Song, Bin-Han Gao**, Department of Radiology, The Central Hospital of Qingdao West Coast New Area, Qingdao 266555, Shandong Province, China**Fu-Shen Han**, Department of Pneumology, The Central Hospital of Qingdao West Coast New Area, Qingdao 266555, Shandong Province, China**Shu-Xin Xiao**, Department of Hematology, The Affiliated Hospital of Qingdao University, Qingdao 266000, Shandong Province, China**Corresponding author:** Shu-Xin Xiao, MD, Chief Physician, Department of Hematology, The Affiliated Hospital of Qingdao University, No. 16 Jiangsu Road, Qingdao 266000, Shandong Province, China. xsxa@sina.com**Abstract****BACKGROUND**

Patients with severe aplastic anemia (SAA) frequently present with inflammatory episodes, and during flared inflammatory episodes, hematopoietic function is further exacerbated. The gastrointestinal tract is the most common site for infectious and inflammatory diseases, and its structural and functional features confer on it the most potent capacity to affect hematopoietic and immune functions. Computed tomography (CT) is a readily accessible approach to provide highly useful information in detecting morphological changes and guiding further work-ups.

AIM

To explore CT imaging presentations of gut inflammatory damage in adult SAA patients during inflammatory episodes.

METHODS

We retrospectively evaluated the abdominal CT imaging presentations of 17

hospitalized adult patients with SAA in search of the inflammatory niche when they presented with systemic inflammatory stress and exacerbated hematopoietic function. In this descriptive manuscript, the characteristic images that suggested the presence of gastrointestinal inflammatory damage and related imaging presentations of individual patients were enumerated, analyzed and described.

RESULTS

All eligible patients with SAA had CT imaging abnormalities that suggested the presence of an impaired intestinal barrier and increased epithelial permeability. The inflammatory damages were concurrently present in the small intestine, the ileocecal region and the large intestines. Some readily identified imaging signs, such as bowel wall thickening with mural stratification (“water holo sign”, “fat holo sign”, intramural gas and subserosal pneumatosis) and mesenteric fat proliferation (fat stranding and “creeping fat sign”), fibrotic bowel wall thickening, “balloon sign”, rugged colonic configuration, heterogeneity in the bowel wall texture, and adhered and clustered small bowel loop (including various patterns of “abdominal cocoon”), occurred at a high incidence, which suggested that the damaged gastrointestinal tract is a common inflammatory niche responsible for the systemic inflammatory stresses and the exacerbated hematopoietic failure in patients with SAA. Particularly, the “fat holo sign” was present in 7 patients, a rugged colonic configuration was present in 10 patients, the adhesive bowel loop was present in 15 patients, and extraintestinal manifestations suggestive of tuberculosis infections were present in 5 patients. According to the imaging features, a suggestive diagnosis of Crohn’s disease was made in 5 patients, ulcerative colitis in 1 patient, chronic periappendiceal abscess in 1 patient, and tuberculosis infection in 5 patients. Other patients were diagnosed with chronic enterocolitis with acutely aggravated inflammatory damage.

CONCLUSION

Patients with SAA had CT imaging patterns that suggested the presence of active chronic inflammatory conditions and aggravated inflammatory damage during flared inflammatory episodes.

Key Words: Aplastic anemia; Computed tomography; Bowel inflammatory damage; Fat holo sign; Balloon sign; Abdominal cocoon

©The Author(s) 2023. Published by Baishideng Publishing Group Inc. All rights reserved.

Core Tip: Patients with severe aplastic anemia frequently present with inflammatory episodes. The gastrointestinal tract is the most common site for infectious and inflammatory diseases, and its structural and functional features confer on it the most potent capacity to affect hematopoietic and immune functions. We retrospectively reviewed the bowel morphological changes on computed tomography in seventeen patients with severe aplastic anemia during flared inflammatory episodes. All patients demonstrated imaging abnormalities that suggested the presence of active chronic inflammatory conditions and aggravated inflammatory damage in the gastrointestinal tract. These inflammatory conditions likely contributed to their systemic inflammatory stresses and exacerbated hematopoietic failure.

Citation: Zhao XC, Xue CJ, Song H, Gao BH, Han FS, Xiao SX. Bowel inflammatory presentations on computed tomography in adult patients with severe aplastic anemia during flared inflammatory episodes. *World J Clin Cases* 2023; 11(3): 576-597

URL: <https://www.wjgnet.com/2307-8960/full/v11/i3/576.htm>

DOI: <https://dx.doi.org/10.12998/wjcc.v11.i3.576>

INTRODUCTION

Aplastic anemia (AA) is the paradigm of hematopoietic failure resulting from the immune-mediated destruction of hematopoietic progenitor cells, leading to heavily suppressed blood cell productivity and peripheral cytopenia. In patients with severe AA (SAA), fulminant infections, frequently in the absence of localized symptoms and signs, and refractory to broad-spectrum antibiotics, are the most common complications and the main causes of death. Infections in SAA are usually attributed to severely impaired granulopoiesis, and it frequently has a poor response to recombinant human granulocyte colony-stimulating factor (rhG-CSF) treatment[1-3]. However, successful treatment of the underlying

infections can significantly improve the hematological profile and even achieve a complete hematological remission in some patients, providing strong evidence that aggravated inflammatory reactions are responsible, at least in a fraction of patients, for the exacerbated hematopoietic suppression[4-6]. Very recently, initiation and perpetuation of AA pathogenesis has been found to be associated with gut inflammatory disorders (GIDs)[7,8]. However, the role of GIDs in AA pathogenesis is overlooked likely due to the high prevalence and good tolerance of GIDs and the low incidence of AA.

The gastrointestinal tract hosts the most enriched and complex microbial community in the human body. Not only pathogenic microbes but also dysbiotic commensal bacteria and various chemical components can compromise the intestinal barrier[9,10]. In the setting of impaired intestinal barrier structure and function, antigens from commensal microbes and undigested food as a source of continuous antigen supply can translocate to the lamina propria, blood, and remote organs and come into intimate contact with host immune cells, thereby initiating and perpetuating autoimmunity[11,12] and amplifying aberrant immune responses[13]. The gastrointestinal tract also hosts the most enriched lymphoid tissues and hence can provide sufficient activated immune cells to sustain exaggerated immune responses. Because the body is constantly confronted with various harmful environmental factors, the gastrointestinal tract is the most common site for infectious and inflammatory diseases[9,10].

Active GIDs, whether as a consequence or as an incentive factor in the process of gut dysbiosis and epithelial damage, can lead to morphological manifestations that can be detected by various imaging modalities. The imaging presentations are usually nonspecific, and arriving at an etiopathological diagnosis usually necessitates the comprehensive analysis of data from clinical, endoscopic, pathological and laboratory investigations, and is frequently dependent on the results of specific laboratory tests and the responses to specific treatments. However, computed tomography (CT) is a readily accessible approach able to provide highly useful information not only in detecting the distribution, extent, degree, and patterns of the gastrointestinal lesions and the adjacent inflammatory changes that prompt a radiological diagnosis but also in guiding further work-ups for pathognomonic diagnosis, identifying complications, evaluating treatment responses and monitoring disease activities in the subsequent follow-ups[14-16]. In this study, we explored the CT imaging manifestations of the gastrointestinal tract in adult patients with SAA during flared inflammatory episodes and showed that all patients had imaging abnormalities suggesting the presence of active chronic gut inflammatory conditions and acutely aggravated inflammatory damages.

MATERIALS AND METHODS

Participants

In this retrospective study, we reviewed the abdominal CT images in 17 hospitalized adult SAA patients who were treated at our center from October 2019 to March 2022, including 8 males and 9 females, with a median age of 55 years (ranging from 34 to 78 years). They were hospitalized due to rapidly exacerbated cytopenia, aggravated fatigue, varying degrees of febrile episodes and elevated inflammatory indices, indicating the presence of systemic inflammatory responses[1-3]. Each patient was definitively diagnosed with SAA for more than 2 years, and the SAA progressed from non-SAA (NSAA) after the patients experienced various accelerating episodes. In addition to supportive care, they were routinely treated with cyclosporine (3-4 mg/kg/d), stanozolol (6-8 mg/d) and eltrombopag (50 mg/d) in the SAA stage, in the absence of any therapeutic responses. In the patients with very SAA (VSAA), recombinant human granulocyte colony-stimulating factor (rhG-CSF, 100-200 µg/d) was added, without an evident increase in granulocytes. Patients who had diseases of portal hypertension, hepatic disease, pancreatic disease, cardiopulmonary disease, heart failure, severe hypoalbuminemia and ischemic enteropathy were excluded, because these diseases can cause stratified bowel wall thickening by blood congestion in the gastrointestinal tract, which may confound the imaging presentations of inflammatory lesions[16-18]. Abdominal CT was performed to search for the inflammatory niche before antibiotic and other treatments.

The modified Camitta criteria were used to assess severity of AA[3]: The diagnostic criteria for SAA were absolute neutrophil count (ANC) $< 0.5 \times 10^9/L$, platelets (Plts) $< 20 \times 10^9/L$, and absolute reticulocyte count (Ret) $< 20 \times 10^9/L$. The diagnostic criteria for VSAA were ANC $< 0.2 \times 10^9/L$ in addition to the above hematological presentations.

Study procedure

CT imaging modalities: Conventional CT was performed for all patients in the search of the inflammatory niche during flared inflammatory episodes. If the conventional CT was sufficient to determine the radiological changes, contrast-enhanced CT was waived in order to reduce the radiation exposure. If the conventional CT was unable to determine the imaging abnormalities due to the difficulty in the discrimination of a massive lesion from contents in the intestinal lumen or due to the suspicion of a massive lesion being malignant, contrast-enhanced CT was performed. Meanwhile, endoscopic examination of the large intestine and ileocecal region was performed. Contrast-enhanced CT was performed in 1 patient in this study. Multiplanar reconstruction was performed for the assessment and

expression of the radiological manifestations.

CT image reviewing process: Each patient's CT images were reviewed, and the imaging abnormalities were collected independently by each of the six authors: Xi-Chen Zhao, Cheng-Jiang Xue, Hui Song, Bin-Han Gao, Fu-Sen Han, and Shu-Xin Xiao. After several rounds of extensive consultation, the imaging abnormalities suggesting the presence of GIDs were decided by the first and corresponding author. In patients with evident chest CT presentations that likely had pathogenic relationships with the bowel inflammatory damages; those chest CT abnormalities were also enumerated and described.

Radiological manifestations suggesting the gut involvement of inflammatory disorders: After careful assessment of the radiographs and after extensive consultations within our research group with reference to the patients' symptoms and signs, the following imaging presentations were considered to have abnormalities suggestive of the presence of GIDs.

First, the criteria for the diagnosis of bowel wall thickening met one of the following criteria[17-21]: (1) Bowel wall thickness greater than 3 mm in adequately distended intestinal segments; (2) bowel wall thickness greater than 4 mm in underdistended intestinal segments; (3) cross-sectional diameter greater than 6 mm in collapsed small intestines; and (4) cross-sectional diameter greater than 5 mm in collapsed large intestines.

The bowel wall thickening may be focal or segmental, symmetrical or asymmetrical, concentric or eccentric, homogeneous or heterogeneous. The following signs were helpful in the identification of the location and extent of the diseased bowel segments: (1) Mesenteric inflammatory changes indicative of transmural inflammation: "fat stranding"[22,23], "creeping fat sign"[24-26] and "comb sign"[27,28]; (2) mural stratification indicative of edematous bowel wall (water halo sign) and submucosal fat deposition (fat halo sign)[17-21]; (3) intramural gas and/or subserosal pneumatosis indicative of aerogenous bacterial proliferation in the bowel wall[14-16]; (4) gas-liquid levels in the intestinal lumen indicative of intestinal dynamical abnormalities; (5) heterogeneity in the bowel wall texture especially with segmentally gas-filled and segmentally liquid-filled intestinal lumen; (6) inflamed diverticulitis; (7) epiploic appendagitis; (8)"empty colon sign" or narrowed bowel lumen[15,16]; (9) adhesive bowel loop, especially with mesenteric inflammatory changes and/or adjacent peritoneal fibrotic thickening ("abdominal cocoon")[29-32]; and (10) rugged colonic configuration, especially with mesenteric inflammatory changes and/or adjacent peritoneal fibrotic thickening.

Second, the "balloon sign" refers to a segment of a paper-thin bowel wall (a highly dilated and thinned bowel segment filled with gas) wrapped by a large cluster of circumferentially distributed hypervascular mesenteric fat stranding[33-36]. The hypervascular mesenteric fat deposition suggests the presence of active chronic transmural inflammatory damage in the diseased intestinal segments[22-26].

Third, peritoneal involvement: Including peritoneal thickening, ascites particularly loculated ascites and peritoneal nodularity.

In the evaluation of bowel inflammatory damage, particular attention was given to imaging abnormalities in the large intestines and ileocecal region, since in these sites, the lymphoid tissues are the most enriched and the microbial community is the most abundant; therefore, inflammatory damage and compromised epithelial integrity in these intestinal segments has the most potent capability to supply sufficient intestine-derived antigens and to activate sufficient immune cells and hence has the most potent capability to affect hematopoietic and immune functions[9,10].

This study was approved by the Institutional Review Board of The Central Hospital of Qingdao West Coast New Area and followed the Declaration of Helsinki (No. 2022-10-08). The requirement for written informed consent was waived by the Review Board since this was a retrospective study, and no information about patient identification was revealed in the manuscript.

Statistical analysis

Categorical data are presented as numbers with percentages, and continuous data are presented as medians with interquartile ranges.

RESULTS

General characteristics of patients

General information, severity of AA, disease duration, complete blood cell count (CBC) results when abdominal CT was performed, major gastrointestinal presentations and suggested radiological diagnosis are listed in Table 1. Seventeen patients (8 men and 9 women) with a median age of 55 years, ranging from 34 years to 78 years were enrolled. The total AA duration ranged from 8 years to 23 years, with a median duration of 13 years, and the total SAA duration ranged from 2 years to 9 years, with a median duration of 5 years. Among all patients, 5 had VSAA. Abdominal tenderness was present in all patients, but abdominal pain was present in only 8 patients, in accordance with the good tolerance of GIDs. Abnormalities in the frequency and property of the feces were present in 11 patients.

Table 1 Clinical characteristics and radiological diagnosis of the studied patients

No.	Sex/age	Hematological diagnosis	Total duration (yr)	SAA duration (yr)	CBC results					Abdominal symptoms	Suggested radiological diagnosis	Extraintestinal abnormalities
					WBC	ANC	Hb	Plts	Rets			
01	M/54	VSAA	23	8	0.66	0.14	44	5	3.17	AP, AT	CAA	
02	M/46	SAA	16	6	1.24	0.55	42	11	6.16	AT	CEC	
03	F/78	VSAA	11	3	0.65	0.17	41	8	1.81	AP, AT	CD	
04	F/38	SAA	17	6	1.62	0.71	45	18	4.18	AP, AT	CEC	
05	M/71	VSAA	14	4	0.57	0.08	42	2	1.92	AT	UC, ATB?	+
06	M/65	SAA	21	8	1.38	0.42	46	13	5.47	AP, AT	CEC	
07	F/52	SAA	11	5	1.48	0.44	53	21	4.62	AT	CEC	
08	M/61	SAA	21	7	1.73	0.77	62	16	2.28	AT	CD, ATB?	+
09	F/55	SAA	9	3	1.17	0.43	48	6	11.75	AT	CEC	
10	M/77	VSAA	8	4	0.42	0.16	40	4	1.78	AT	CD	
11	M/57	SAA	12	2	1.14	0.36	45	14	6.32	AP, AT	CEC	
12	F/48	SAA	12	6	0.92	0.44	40	3	2.08	AT	CD	
13	F/34	SAA	18	7	0.92	0.31	62	7	1.59	AP, AT	ATB?	+
14	F/40	SAA	13	4	0.86	0.27	44	2	6.03	AP, AT	CD	
15	F/42	SAA	20	9	0.82	0.39	51	18	2.14	AT	CEC	
16	M/68	VSAA	10	3	0.47	0.14	39	6	3.44	AT	CEC, ATB?	+
17	F/36	SAA	11	3	1.38	0.31	46	9	8.41	AP, AT	ATB?	+

M: Male; F: Female; SAA: Severe aplastic anemia; VSAA: Very-severe aplastic anemia; WBC: White blood cells ($\times 10^9/L$); CBC: Complete blood cell count; WBC: White blood cell count; ANC: Absolute neutrophil count ($\times 10^9/L$); Hb: Hemoglobin (g/L); Plt: Platelets ($\times 10^9/L$); Ret: Absolute reticulocyte count ($\times 10^9/L$); AP: Abdominal pain; AT: Abdominal tenderness; CAA: Chronic appendiceal abscess; CEC: Chronic enterocolitis; ATB: Abdominal tuberculosis; CD: Crohn's disease; UC: Ulcerative colitis.

CT imaging abnormalities reflecting gut involvement of inflammatory conditions

Characteristic images are enumerated, analyzed and described in the Discussion section. All patients recruited in this study presented with evident imaging abnormalities that suggested the presence of inflammatory damages in the gastrointestinal tract. Noticeably, inflammatory involvement of the large intestine and the ileocecal region was present in all patients. Inflammatory lesions were also present in the small intestine in all patients, suggesting that the inflammatory pathogenesis was most likely initiated at the proximal gastrointestinal tract. According to the imaging features, a suggestive diagnosis

of Crohn's disease was made in 5 patients, ulcerative colitis in 1 patient, chronic periappendiceal abscess in 1 patient, and tuberculosis infection in 5 patients. Other patients were diagnosed with chronic enterocolitis with acutely aggravated inflammatory damage. The suggested radiological diagnosis is listed in Table 1.

DISCUSSION

The severity of cellular immune-mediated hematopoietic suppression in patients with AA commonly fluctuates in parallel with the waxing and waning of physical and mental stresses, and these stresses are obviously driven by active chronic inflammatory conditions and their recurrently aggravated episodes. In flared inflammatory episodes, blood cell production is heavily suppressed, and cytopenia worsens. With effective treatment of the inflammatory episodes, blood cell productivity can be significantly improved. Along with the increased frequency of and decreased intervals between these inflammatory episodes, patients eventually enter into an advanced stage, in which immune-mediated hematological damage is exacerbated and the sensitivity to previous effective treatments is lost[1,2,37,38].

This is not surprising because the blood cells themselves are immune cells, and their production is regulated largely in response to a variety of microbial attacks. When confronting an acute and limited infection, host hematopoiesis skews its proliferation and differentiation toward the production of innate immune cells to fight against the invading microbes at the expense of reduced self-renewal capacity[39, 40]. After the infected pathogens are cleared out, the activated host immune system quickly returns to the homeostatic state, and the skewed blood cell production ends. However, in the setting of active chronic inflammatory conditions or overwhelming infections, host hematopoiesis can be heavily suppressed and exhausted due to prolonged and exaggerated immune responses and the subsequently overproduced proinflammatory mediators[41-43], resulting in heavily decreased marrow cellularity and increased peripheral cytopenia in genetically susceptible subjects, which are the characteristic morphological and immunological changes seen in AA[1-3]. The sustenance of an active inflammatory condition in which the degree and duration of immune responses are sufficient to induce severe aplastic cytopenia critically necessitates sufficient activated immune cells and a continuous antigen supply.

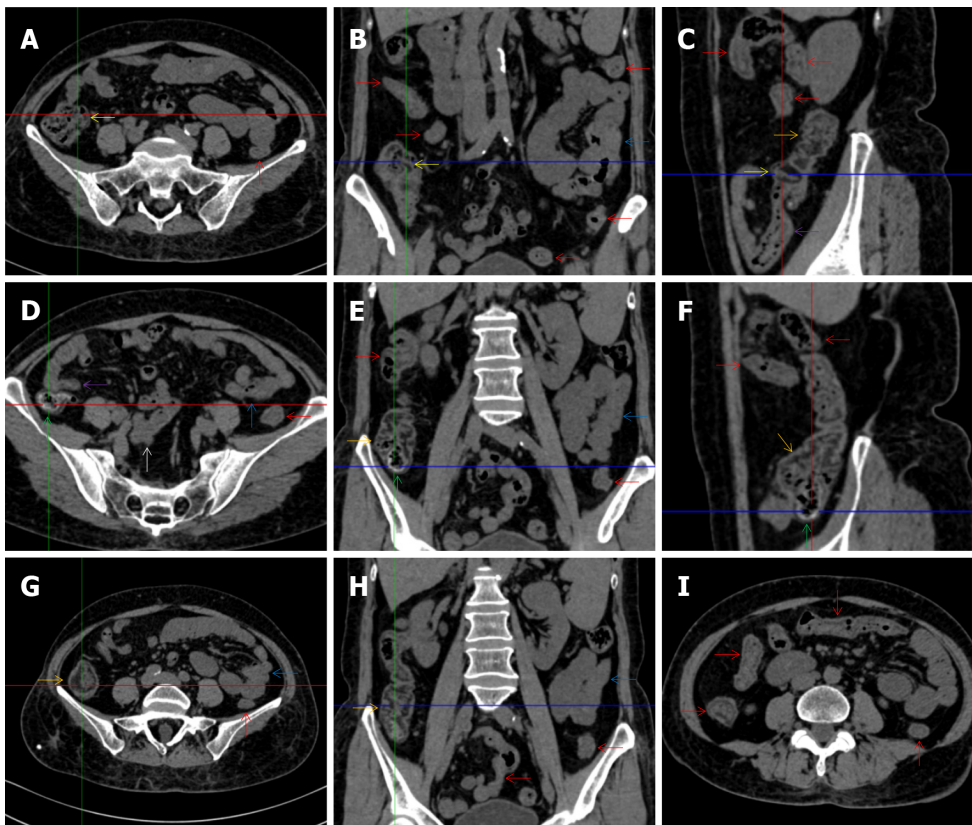
The gastrointestinal tract provides the largest interface bridging the host neuro-endocrine-immune system with environmental factors and is constantly confronted with a variety of environmental challenges. The gastrointestinal tract also hosts the body's most abundant gut-associated lymphoid tissues and microbial community[9,10]. These structural and functional characteristics make the gastrointestinal tract the most vulnerable site for pathogen invasion and chemical injuries and the most common source of a continuous antigen supply. Therefore, the gastrointestinal tract becomes the most important site for pathological interactions between host immune cells and pathogenic antigens.

The gastrointestinal tract is the most common site for chronic and active inflammatory niches not only due to various pathogenic microbial attacks and chemical injuries but also due to dysbiotic commensal microbes and autoimmunity. Such abundant lymphoid tissues and microbial communities confer on the gastrointestinal tract the ability to provide sufficient activated immune cells and a continuous antigen supply and thereby have the most potent capacity to continuously release excessive proinflammatory cytokines.

Under chronic and active inflammatory conditions, upregulated human leukocyte antigen and pattern recognition receptors on hematopoietic progenitors enhance their responsiveness to pathogenic stimulation[44-46], and upregulated Fas molecules accelerate their apoptotic cell death[45], eventually resulting in the exhaustion of hematopoietic progenitor cells. The severity of GIDs is largely affected by changes in a variety of environmental factors, such as food supplements[47-49], antibiotic abuse[50,51], mental stresses[52,53] and pathogen invasion, leading to the fluctuant property of GIDs, in accordance with the fluctuant property of AA.

AA has been reported to be associated with gut inflammatory diseases, including inflammatory bowel disease, celiac disease and neutropenic enterocolitis[8]. In our previously reported case, intermittent treatments with a gut-cleansing preparation achieved reproducible hematological remissions, providing direct evidence for the role of GIDs in the initiation and perpetuation of AA pathophysiology[4]. Merely gluten-free diets[5] or resection of diseased intestinal segments[6] can achieve excellent hematological improvement, providing convincing evidence that GIDs play an indispensable role in the sustenance of AA pathophysiology.

In this pathogenic process, impaired intestinal integrity and increased epithelial permeability play pivotal roles[11,12]. These GID-associated morphological changes could be detected by various imaging modalities. Abdominal CT is a readily accessible and highly efficient imaging modality for detecting morphological changes in the gastrointestinal tract[14-16,19,20]. In this study, we explored the abdominal imaging presentations in patients with SAA in search of the inflammatory niche when the patients presented with systemic inflammatory stresses. We selected patients with SAA experiencing flared episodes because during this stage, morphological changes due to the gut inflammation are probably more serious and hence more easily identified by radiological examination.

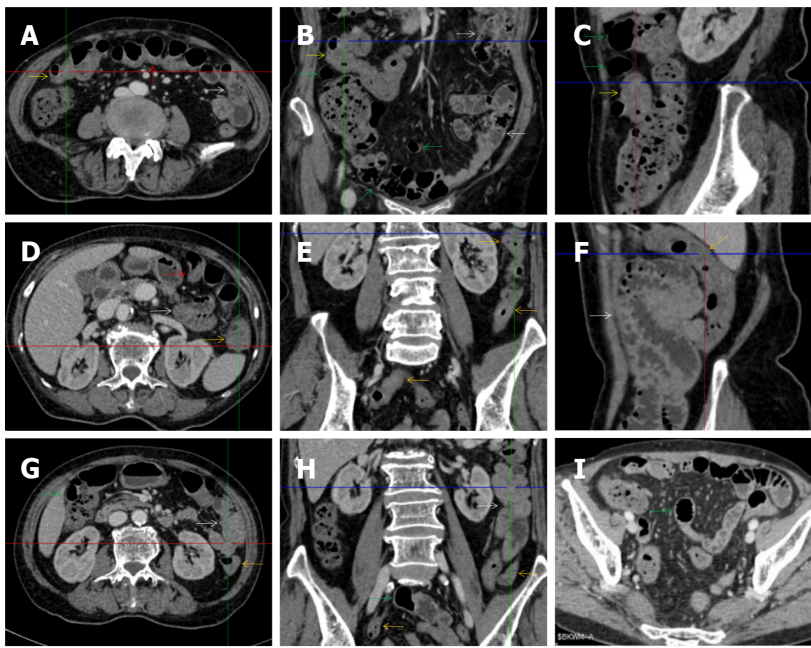


DOI: 10.12998/wjcc.v11.i3.576 Copyright ©The Author(s) 2023.

Figure 1 Characteristic images of case 4. A-C: Characteristic images of the ileocecal region. The ileocecal valve (yellow arrows), the proximal ascending colon (orange arrows) and the terminal ileum (purple arrows) were significantly thickened and stratified by submucosal fat deposition, forming the so-called “fat halo sign”. From the distal ascending colon to the sigmoid colon (red arrows), the wall was thickened and stratified with “water halo sign”. The small intestine was heterogeneous in bowel wall texture, and gas-filled in some segments and liquid-filled in other segments, and a segment of adhesive bowel loop was found in the middle jejunum (blue arrows); D-F: Characteristic images of the ascending colon. The irregular contour and the fibrotic thickening of the mucosal folds made the colonic configuration rugged. The mucosa of the cecum and the appendiceal root was fibrously thickened (green arrows), and the appendix was gas-filled. Thickened omentum surrounded the ileocecal region and the ascending colon. A segment of adhesive bowel loop was found in the proximal ileum (a white arrow). The mucosa of the proximal ileum in the adhered bowel loop was fibrotically thickened, with mesenteric fat deposition and adjacent peritoneal thickening forming the so-called “abdominal cocoon”; G and H: Typical fat halo sign in the ascending colon. The “fat halo sign” was more typical in the middle ascending colon; I: Thickened and stratified larger intestine. From the distal ascending colon to the sigmoid colon (red arrows), the wall was thickened and stratified by edematous submucosal tissues, forming the so-called “water halo sign”. In some segments, the colon was emptied. Paracolic fat stranding was present from the cecum to the sigmoid colon. The disproportionately less severe paracolic fat stranding suggested that the edematous colon most likely occurred during an acute episode.

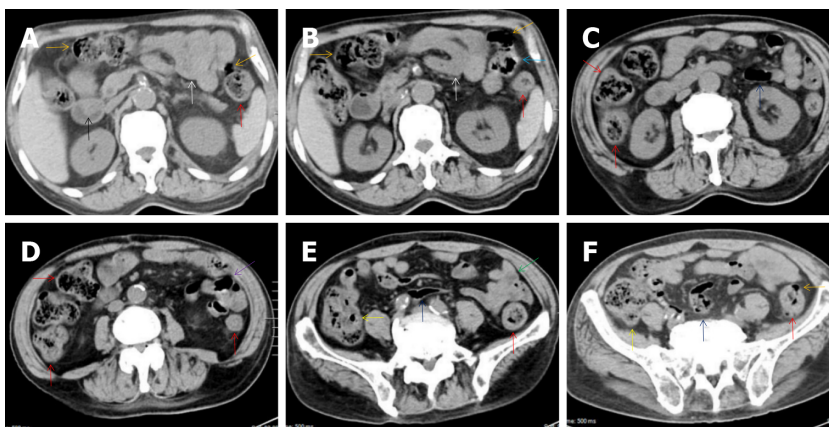
In the evaluation of abdominal CT imaging abnormalities, particular attention has been given to inflammatory abnormalities in the ileocecal region and the colonic segments because they host the most enriched microbial community and lymphoid tissues[9,10,19]; therefore, inflammatory diseases and compromised intestinal barriers in these bowel segments have the most potent capacity to provide sufficient intestine-derived antigens and activated immune cells to affect hematopoietic and immune functions irrespective of whether they are primary damage or secondary to dysbiotic gut microbiota. As demonstrated by this study, all patients with SAA during flared inflammatory episodes had evident morphological abnormalities that could reflect the presence of a severely damaged intestinal structure and function in the ileocecal region and the colonic segments. All patients also presented with inflammatory damages in the proximal small intestine, suggesting that inflammatory damages in the upper gastrointestinal tract led to the inflammatory damages in the downstream intestinal segments, probably by altering the gut microbial composition[54-56]. In the following sections, we described the characteristic CT imaging findings in each patient in the category of readily identified morphological presentations.

All patients demonstrated CT imaging abnormalities that suggested the presence of gut inflammatory damage in the large intestine. Colonic wall thickening with mural stratification, intramural gas and paracolic fat stranding is the common presentation of colonic involvement of inflammatory damage. A stratified bowel wall can be caused by submucosal fat deposition (fat halo sign) or submucosal edematous tissues (water halo sign)[17-19]. The water halo sign was present in 8 patients [Figure 1 (case 4), Figure 2 (case 3), Figure 3 (case 6), Figure 4 (case 9), Figure 5 (case 15), Figure 6 (case 2), Figure 7 (case 1), and Figure 8 (case 12)], commonly accompanying intramural gas and subserosal pneumatosis, which indicated the presence of aerogenous bacterial proliferation in the colonic wall irrespective of primary



DOI: 10.12998/wjcc.v11.i3.576 Copyright ©The Author(s) 2023.

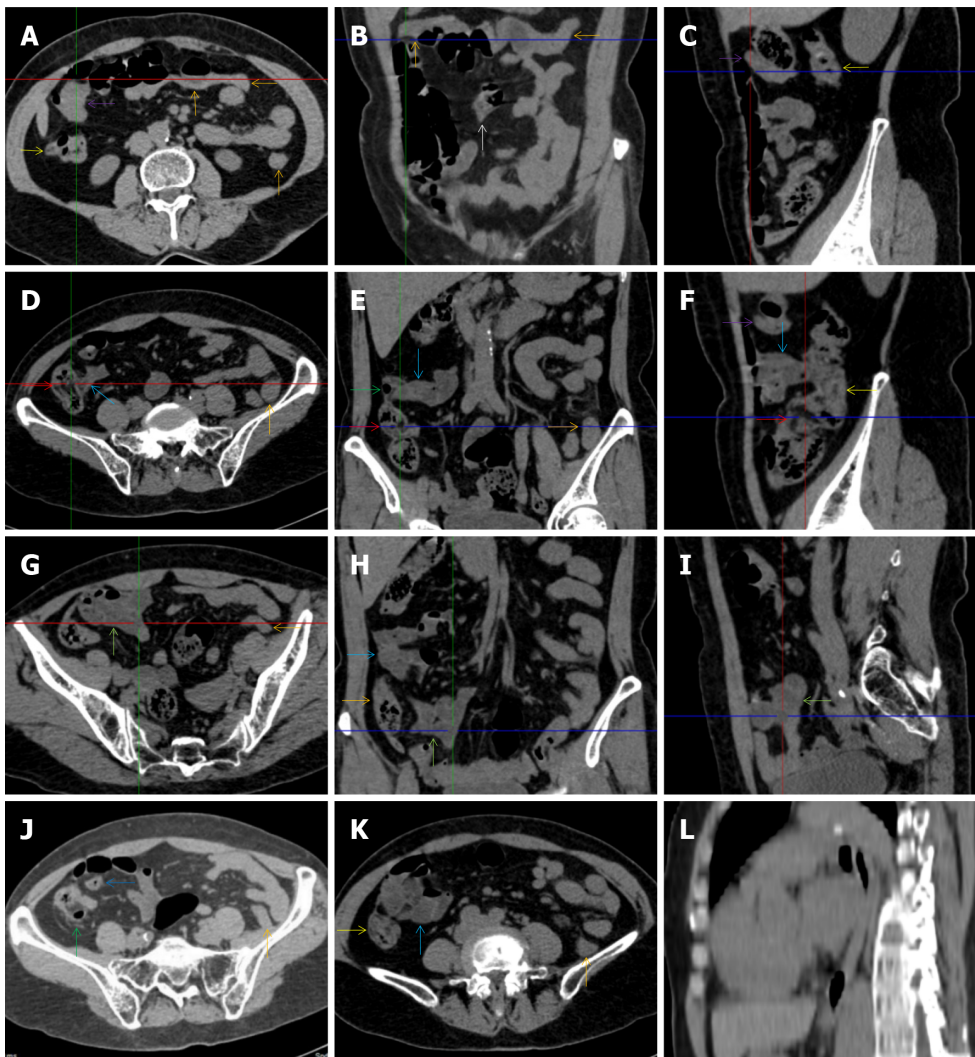
Figure 2 Characteristic images of case 3. A-C: Characteristic images of the thickened transverse colon. The segmentally thickened, stratified (water holo sign) and emptied colon with paracolic fat stranding was present in the hepatic flexure (yellow arrows) in which an inflamed polypoid lesion was found on endoscopic examination, followed by the asymmetrically thickened wall and gas-filled lumen of the transverse colon (red arrows) in which the colonic villi were absent; D-F: Characteristic images of the thickened descending colon. The wall of the descending and sigmoid colon was thickened and stratified with mesenteric fat stranding (orange arrows), with the most striking segment being in the splenic flexure; G and H: Characteristic images of an adhesive bowel loop. While the ileum was gas-filled and distended (green arrows), the adhesive jejunal loop (white arrows) was heterogeneous in bowel wall texture and liquid-filled with multiple gas-liquid levels and accrescent plica. Increased mesenteric fat and vasculature were adjacent to the adhered jejunal loop; I: Characteristic image of a balloon sign. Clustering and hypervascular mesenteric fat proliferation wrapped a segment of paper-thin ileum, forming the so-called "balloon sign". Balloon sign was also present in the hepatic flexure.



DOI: 10.12998/wjcc.v11.i3.576 Copyright ©The Author(s) 2023.

Figure 3 Characteristic images of case 6. A and B: Characteristic images of the upper abdomen. Several inflamed diverticula (orange arrows) were present in the colonic segments. In the duodenum-jejunum junction (a blue arrow), the bowel wall was fibrotically thickened and the lumen was gas-filled. In the bulb part of the duodenum, a polypoid mass (a black arrow) protruded into the lumen. A segment of adhesive jejunal loop was present in the proximal jejunum (white arrows); C and D: Characteristic images of the thickened colon. The wall from the cecum to the descending colon was significantly thickened with mural stratification, intramural gas and pericolic fat stranding. A segment of adhesive bowel loop was present in the middle jejunum (a purple arrow) in which the bowel wall was asymmetrically thickened and the lumen was gas-filled with particularly prominent mesenteric fat stranding; E: Characteristic images of the ileocecal region. Stratified thickening of the ileocecal valve and the terminal ileum was gas-filled (yellow arrows). The third segments of adhesive bowel loop were present in the distal jejunum (a green arrow); F: Characteristic image of a balloon sign. The sigmoid colon was dilated and the wall was paper-thin (navy blue arrows), with clustering pericolic fat stranding forming the so-called "balloon sign".

infection or infection secondary to dysbiotic microbiota, acute episodes or chronic damage[22,23]. The fat holo sign which suggested the existence of active chronic gut inflammation was detected in 7 patients [Figure 1 (case 4), Figure 9 (case 13), Figure 4 (case 9), Figure 10 (case 11), Figure 11 (case 17), Figure 7 (case 1), and Figure 12 (case 16)]. In these 7 patients, the fat holo sign was located in the

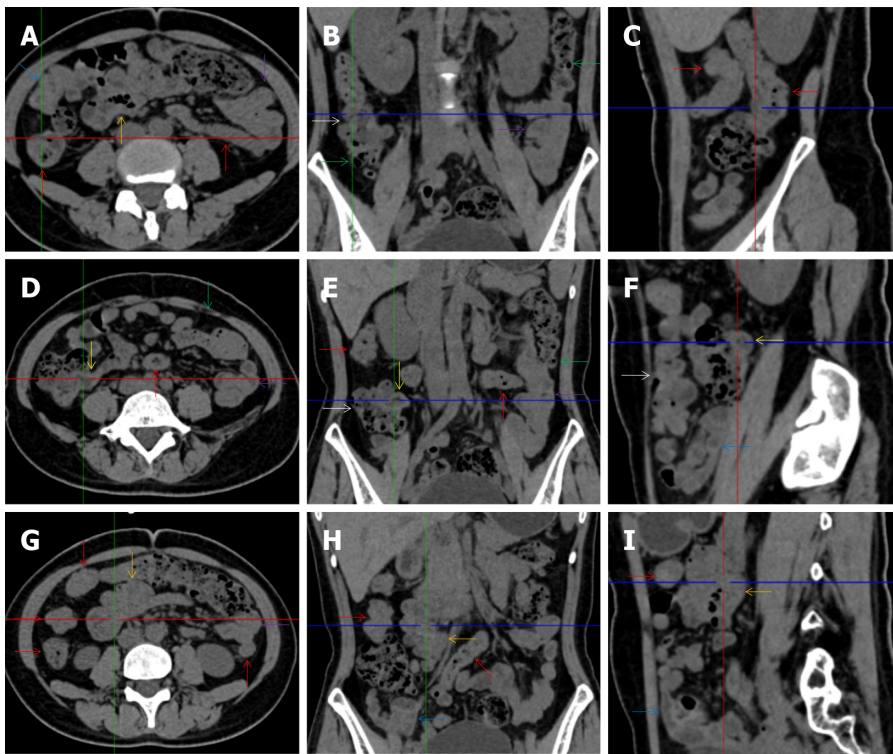


DOI: 10.12998/wjcc.v11.i3.576 Copyright ©The Author(s) 2023.

Figure 4 Characteristic images of case 9. A-C: Characteristic images of an empty colon sign. The segmentally wall-thickened, stratified and emptied colon in the hepatic flexure (purple arrows) followed by the collapsed transverse (adjacent to the dilated ileum in which gas-liquid levels could be recognized) and descending colon (orange arrows), forming the so-called “empty colon sign”. A short segment of asymmetrically thickened wall was present in the proximal ileum (a white arrow), around which the hypervascular fat stranding was especially prominent, distal to which the ileal lumen was gas-filled, and proximal to which the ileal lumen was liquid-filled; D-F: Characteristic images of the ileocecal region. The ileocecal valve and the terminal ileum were thickened and stratified by submucosal fat deposition (red arrows). Omental thickening was especially prominent in the ileocecal region. The wall of the ascending colon was thickened and, in some segments, stratified with submucosal fat deposition, and in other segments, stratified with submucosal edematous tissue (yellow arrows). Several inflamed diverticula (green arrows) were present in the cecum and ascending colon. The distal ileum was strictured (blue arrows), proximal to which the ileal lumen was liquid-filled; G-I: Characteristic images of adhesive bowel loops. The fibrotic mucosa and liquid-filled lumen of the adhesive bowel loops were present in the proximal ileum (powder blue arrows) and distal ileum (jade-green arrows); J: Characteristic image of a balloon sign. A large cluster of circumferentially distributed hypervascular fat stranding wrapped a segment of the dilated lumen and paper-thin bowel wall of the sigmoid colon, forming the so-called “balloon sign”. An inflamed diverticula was present in the cecum, with strikingly thickened omentum (a green arrow); K: Characteristic image of an adhesive bowel loop in the proximal ileum. A segment of adhesive bowel loop in the proximal ileum, together with the fibrotically thickened peritoneum, formed the so-called “abdominal cocoon”; L: Characteristic image of esophagus. Hypertrophic lesions presented in two segments of the esophagus, together with the inflammatory lesions in the jejunum suggesting that the initiating factor in the upper gastrointestinal tract affected the functions of the downstream intestinal segments.

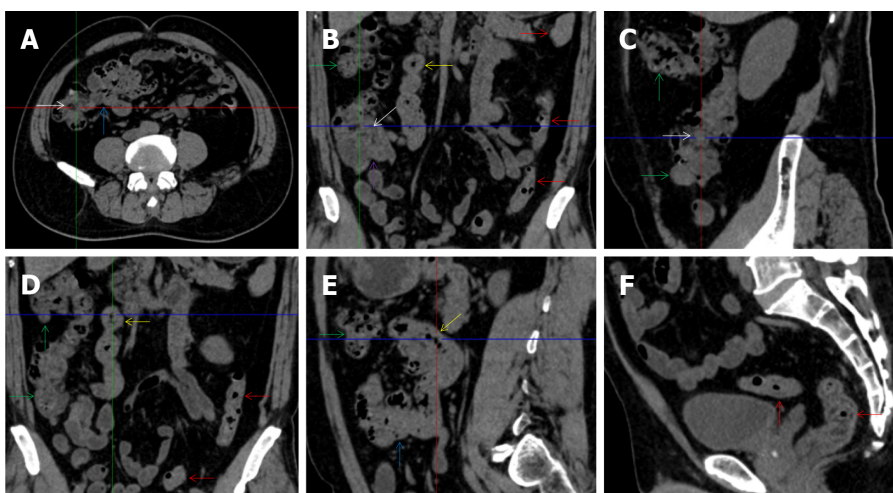
ileocecal region and proximal ascending colon.

The “balloon sign” is characterized by circumferentially distributed clustering of hypervascular mesenteric fat proliferation wrapping a short segment of highly distended paper-thin bowel wall[33, 34]. The “balloon sign” can also be seen in a large subserosal pneumatosis[35,36]. The circumferentially distributed clustering of hypervascular fat proliferation suggests the presence of an active chronic inflammatory condition in diseased intestinal segments. The balloon sign was present in 7 patients. The paper-thin bowel wall can be the wall of either the small or large intestine. In Figure 2 (case 3), the paper-thin bowel wall was present in the proximal ileum. In Figure 13 (case 14), the paper-thin bowel wall was present in the ascending colon. In Figure 11 (case 17), the paper-thin bowel wall was present in the hepatic flexure. In Figure 3 (case 6), Figure 4 (case 9), Figure 8 (case 7) and Figure 14 (case 8), the paper-thin bowel wall was present in the sigmoid colon.



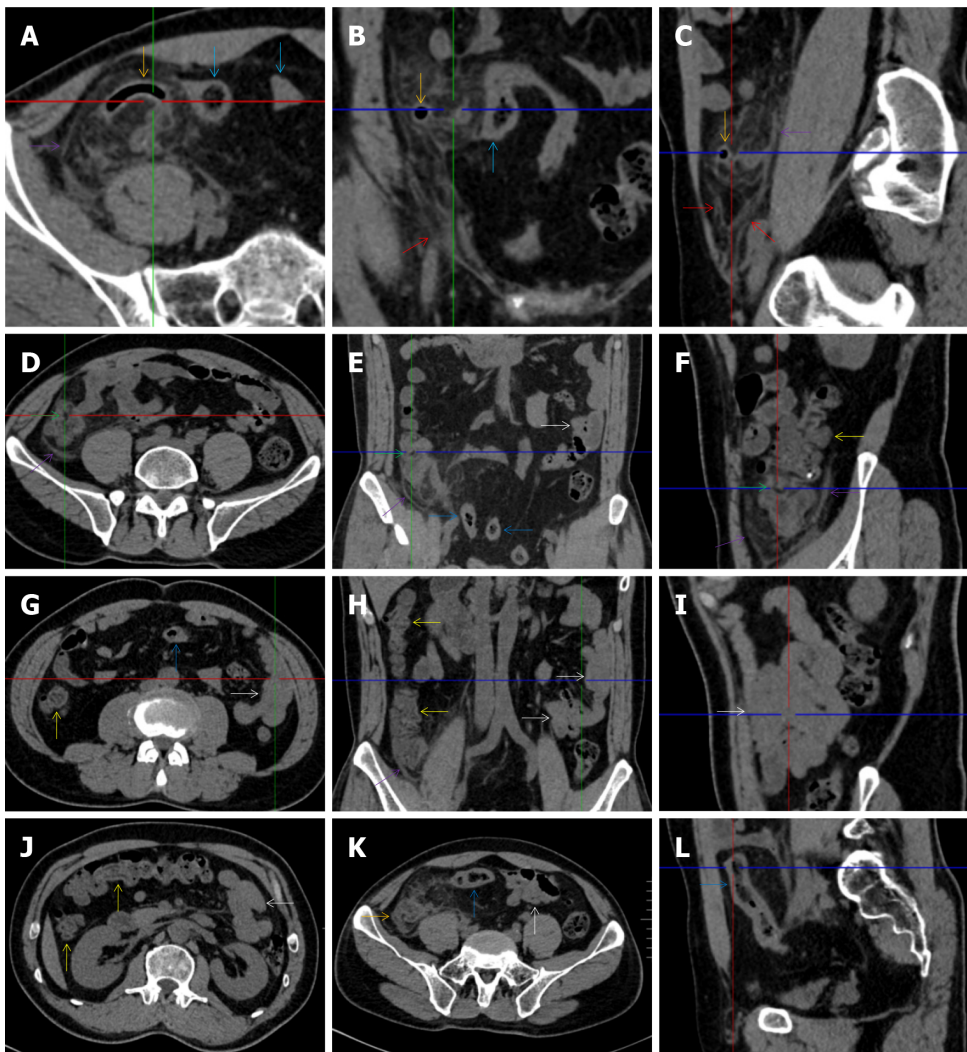
DOI: 10.12998/wjcc.v11.i3.576 Copyright ©The Author(s) 2023.

Figure 5 Characteristic images of case 15. A-C: Characteristic images of the ascending colon. The ascending colon was rugged with omental thickening and paracolic fat stranding, and the colonic wall was thickened with mural stratification and intramural gas (white arrows). From the hepatic flexure to the sigmoid colon (red arrows), the bowel wall was thickened and stratified with several inflamed diverticula (green arrows) in these colonic segments. Three segments of adhesive bowel loops were visualized: one in the distal ileum (blue arrows), the other two in the middle ileum (orange arrows) and the jejunum (purple arrows); D-F: Characteristic images of the ileocecal region. The ileocecal valve and the terminal ileal wall were fibrotically thickened (yellow arrows), proximal to which the ileal lumen was liquid-filled; G-I: Characteristic images of the adhesive bowel loops in the middle and distal ileum. The bowel loop in the middle ileum was adhered and clustered (orange arrows), with the bowel wall being highly heterogeneous in texture and the mucosa being hyperdense. The bowel loop in the distal ileum was adhered, the lumen was liquid-filled, and the bowel wall was fibrotically thickened, together with the fibrotically thickened peritoneum forming the so-called “abdominal cocoon” (blue arrows).



DOI: 10.12998/wjcc.v11.i3.576 Copyright ©The Author(s) 2023.

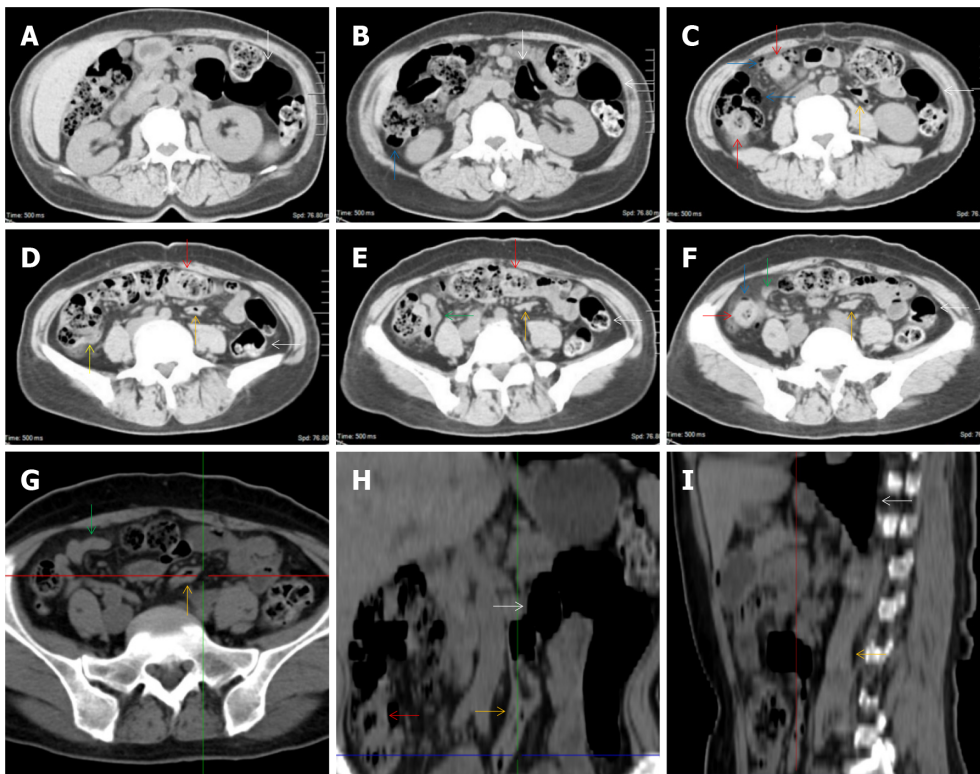
Figure 6 Characteristic images of case 2. A-C: Characteristic images of the ileocecal region. The ileocecal valve and the terminal ileal wall were thickened and stratified (white arrows), the ileal mucosa was hyperdense and the ileal lumen was liquid-filled. The adhered and clustered distal ileum and cecum with the fibrotically thickened peritoneum (a purple arrow) formed the so-called “abdominal cocoon”; D and E: Characteristic images of the ascending colon and the adhesive bowel loops. In the ascending colon (green arrows), the wall was thickened and stratified with “water halo sign”, the mucosa was hyperdense and the configuration was rugged, with paracolic fat stranding, omental thickening and subserosal pneumatoses. The wall of the descending and sigmoid colon (red arrows) was also thickened and stratified. In two segments of the adhesive bowel loop (blue arrows and yellow arrows), the bowel wall was heterogeneously thickened and the lumen was gas-filled, suggesting the presence of heterogeneity in small bowel wall texture; F: A particularly striking edematous segment was present in the rectum.



DOI: 10.12998/wjcc.v11.i3.576 Copyright ©The Author(s) 2023.

Figure 7 Characteristic images of case 1. A-C: Characteristic images of the ileocecal region. A massive cluster of fat stranding that was wrapped by the strikingly thickened omentum (purple arrows) was centered on the homogeneously wall-thickened and gas-filled appendix (orange arrows), leading to the diagnosis of a chronic periappendiceal abscess. The periappendiceal inflammatory changes extended to the scrotum along the inguinal canal (red arrows). In the adjacent sigmoid colon, the wall was thickened and stratified with the water halo sign, and the lumen was gas-filled (blue arrows); D-F: Characteristic images of the ascending colon. The ileocecal valve was thickened and strictured (green arrows), proximal to which the ileal lumen was liquid-filled. Bowel wall thickening with irregular mucosal folds, emptied lumen, mural stratification (fat halo sign) and paracolic fat stranding that was disproportionately less severe than the severity of the colonic wall thickening was present in the ascending colon (yellow arrows). In the descending colon, the wall was also fibrotically thickened; G-I: Characteristic images of an adhesive bowel segment. A segment of adhesive bowel loop with fibrotic bowel wall thickening, peritoneal thickening and hypervascular mesenteric fat stranding was present in the jejunum (white arrows), together with the segmentally gas-filled, segmentally liquid-filled jejunal lumen, suggesting the inflammatory involvement of the upper gastrointestinal tract; J: Characteristic image of the thickened transverse colon. Bowel wall thickening with emptied lumen, mural stratification (water halo sign) and paracolic fat stranding that was disproportionately less severe than the severity of the colonic wall thickening was present in the transverse colon, suggesting the involvement of a transmural inflammatory condition; K and L: The thickened and stratified sigmoid colon. Of the sigmoid colon adjacent to the massive inflammatory lesion, the wall was thickened and stratified with the water halo sign, and the lumen was gas-filled.

The “empty colon sign” refers to a colonic segment in which any contents are absent, usually in a segmentally wall-thickened colon or following a focally wall-thickened colon. Malignant masses are the most common cause. However, inflammatory diseases can also cause empty colon signs, especially in segmental thickening of the colonic wall with edematous submucosal tissues and prominent mesenteric fat stranding[15-18]. In this study, 6 patients presented with an empty colon sign. In **Figure 9** (case 13), the empty colon sign was exhibited a thickened, stratified and emptied colonic segment in the hepatic flexure, followed by the collapsed proximal transverse colon. In **Figure 4** (case 9), the collapsed transverse and descending colon followed the segmentally wall-thickened colon in the hepatic flexure, and endoscopic examination later demonstrated a polypoid lesion in the diseased colonic segment. In **Figure 7** (case 1), the empty colon sign was exhibited as a long segment of the thickened, stratified and emptied ascending and proximal transverse colon. In **Figure 1** (case 4), **Figure 2** (case 3) and **Figure 5** (case 15), the empty colon sign was exhibited a segmentally thickened, stratified and emptied colon in the hepatic flexure.



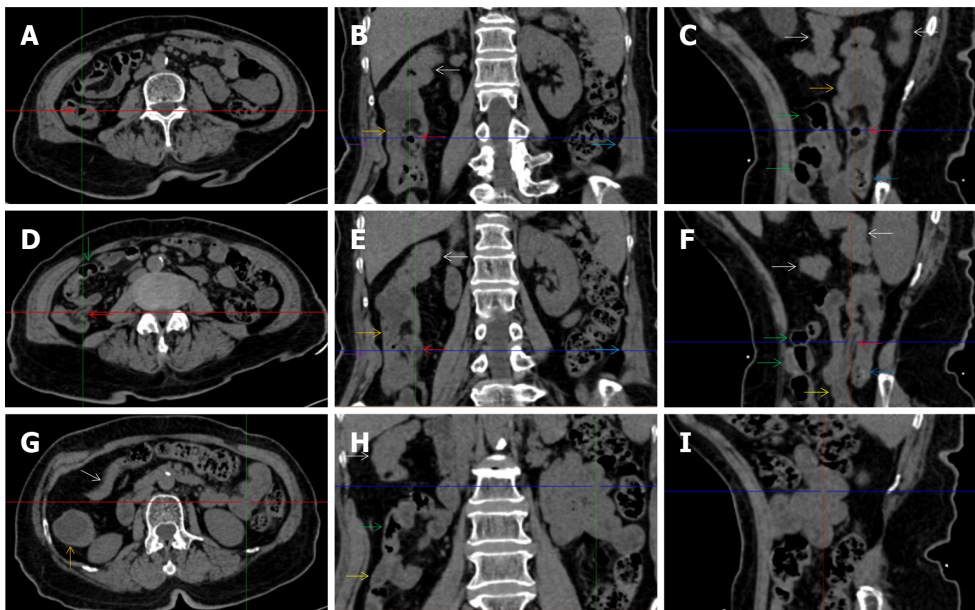
DOI: 10.12998/wjcc.v11.i3.576 Copyright ©The Author(s) 2023.

Figure 8 Characteristic images of case 7. A-F: Characteristic images of the ileocecal region and the large colon. The ileocecal valve was thickened and stratified (yellow arrow). The distal ileum was thickened and strictured (green arrows) with a large cluster of misty exudative lesions surrounding the cecum and distal ileum, and the proximal small intestine was liquid-filled with multiple gas-liquid levels. From the cecum to the distal descending colon, the mucosa and the villi were hyperdense, with several focally wall-thickened and stratified colonic segments (red arrows) and several inflamed diverticula (blue arrows). An obstructively thickened segment of the sigmoid colon (orange arrows) with prominent paracolic hypervascular fat stranding was distal to the remarkably distended lumen and paper-thin bowel wall of the sigmoid colon (white arrows); G-I: Reconstructed images of the obstructively thickened sigmoid colon. From the reconstructed images, the obstructively thickened segment of the sigmoid colon (orange arrows) and the proximal distended sigmoid colon (white arrows) were better visualized. The misty exudative lesions and the surrounded cecum and distal ileum were also better visualized (green arrows).

The “creeping fat sign” represents an imaging presentation in which proliferated fat deposition leads to the widening of the bowel loop[24]. The appearance of the creeping fat sign signifies the presence of chronic transmural inflammation in diseased intestinal segments[16,18,24,25]. In Figure 15 (case 10), the silt-like fat deposition led to the widening of the small bowel loop. In the ileal segment, the wall was thickened, and the lumen was dilated. In Figure 14 (case 8), similar imaging features were shared with those in Figure 15 (case 10). However, Figure 14 (case 8) presented concomitantly with infectious lesions in the pleura, indicative of the reactivation of old tuberculosis.

Diffused bowel inflammatory damage in Crohn’s disease predominantly affects the small intestine, and the ileocecal valve and large intestine are commonly involved. The “creeping fat sign” is the characteristic imaging presentation in the diagnosis of Crohn’s disease[24,25]. In Figure 15 (case 10), the “creeping fat” manifested as silt-like fat deposition. However, most patients manifested perienteric hypervascular fat proliferation wrapping the fibrotically thickened wall and dilated lumen of the ileal segment. Four patients (cases 8, 9, 12, and 14) were found to have this radiological feature. In Figure 14 (case 8), this form of creeping fat was present in the distal jejunum, whereas in the other 3 patients [Figure 15 (case 9), Figure 16 (case 12) and Figure 13 (case 14)], creeping fat was present in the ileum. They also presented with other forms of inflammatory changes in the small and large intestines.

While the diffuse bowel inflammatory lesions of Crohn’s disease predominate in the small intestine, the bowel inflammatory lesions of ulcerative colitis predominate in the colon. Fibrotic thickening of the colonic wall is a common imaging presentation, usually with striking paracolic hypervascular mesenteric fat proliferation, indicating chronic lesions in nature, different from those of acute colonic infectious diseases[15-19]. The ileocecal region and small intestine are commonly involved in various forms of inflammatory damages. These imaging features were present in Figure 17 (case 5). In addition to fibrotic thickening of the colonic wall and the dilated colonic lumen, peritoneal thickening and loculated ascites in the iliac fossa and pelvic cavity indicated peritoneal involvement of inflammatory lesions. The hypertrophic lesion in the pleura with pleural effusion suggested the presence of tuberculosis infection. These imaging features indicated that tuberculosis infection likely initiated the gut inflammatory condition in this case.

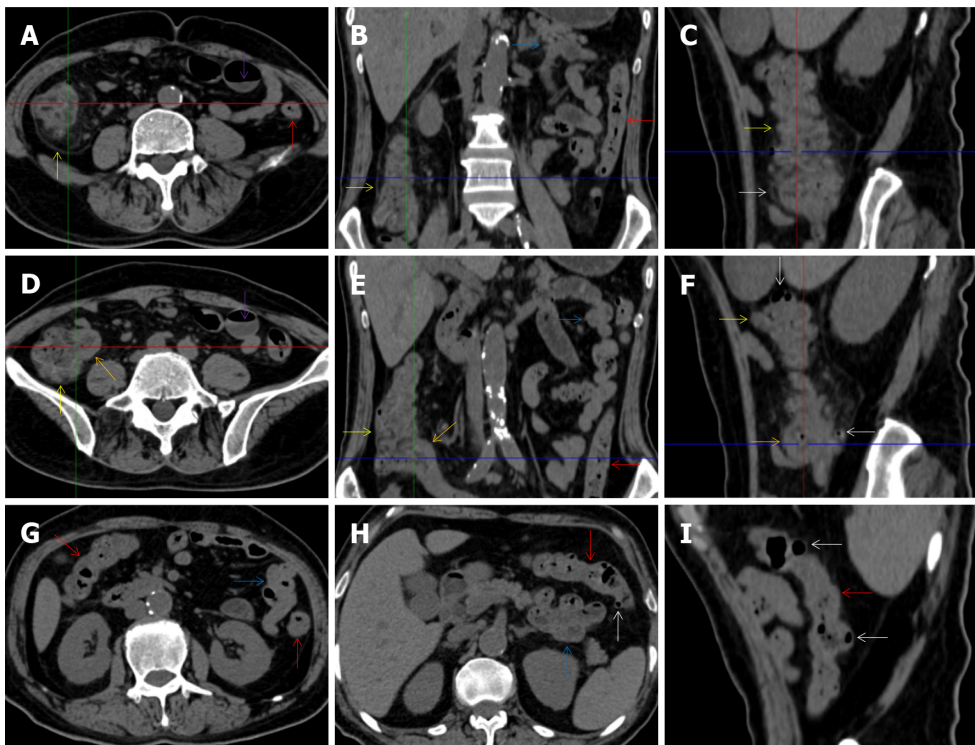


DOI: 10.12998/wjcc.v11.i3.576 Copyright ©The Author(s) 2023.

Figure 9 Characteristic images of case 13. A-C: Characteristic images of the ileocecal valve and ascending colon. There was edematous fat deposition around the ileocecal valve and the terminal ileum, forming the so-called “fat halo sign”. A massive necrotic lesion in the colonic wall was adjacent to the edematous fat deposition, and the serosal colonic wall was hypertrophically thickened (orange arrows). The adjacent parietal peritoneum (purple arrows) and the left parietal peritoneum (navy blue arrows) were also hypertrophically thickened. The mucosa of the cecum was fibrotically thickened (blue arrow); D-F: Characteristic images of the distal ileum. Strictured thickening of the ileocecal valve and terminal ileum (red arrows) led to the distal ileum being liquid-filled. Proximal to the liquid-filled distal ileum (yellow arrows) was the asymmetrical wall-thickened and gas-filled ileum (green arrows). Heterogeneity of the small bowel wall was observed; G-I: Characteristic images of an “abdominal cocoon”. A segment of adhesive bowel loop was present in the middle jejunum, together with the fibrotically thickened bowel and peritoneal involvement forming the so-called “cauliflower sign”. Edematously thickened colonic wall and emptied colonic lumen were present from the proximal ascending colon to the hepatic flexure, followed by a segment of the collapsed transverse colon (white arrows), forming the so-called “empty colon sign”.

Marked irregular mucosal contour and fibrotically thickened mucosal folds of the large intestine, commonly with colonic wall thickening and subserosal pneumatosis, makes the colonic configuration rugged. This rugged colonic configuration especially with peritoneal thickening could suggest an existence of active and chronic inflammatory conditions in diseased colonic segment. It commonly occurs in the ascending colon and coexists omental involvement and pronounced paracolic fat stranding. This easily recognized imaging presentation is highly useful in the identification of colonic inflammatory damages which is distinguishable from edematous thickening of the colonic wall with disproportionately less severe paracolic fat stranding in acute enterocolitis[14-18]. In patients presented with this imaging presentation, inflammatory lesions also involved other colonic segments, the ileocecal region and small intestine. The rugged configuration of the ascending colon presented in 10 patients [Figure 1 (case 4), Figure 2 (case 3), Figure 4 (case 9), Figure 5 (case 15), Figure 10 (case 11), Figure 6 (case 2), Figure 11 (case 17), Figure 7 (case 1), Figure 14 (case 8) and Figure 12 (case 16)], suggesting that it is common imaging presentations in patients with SAA, in accordance with the high prevalence of inflammatory and infectious diseases in the ileocecal region and the proximal ascending colon.

The “adhesive bowel loop” refers to a segment of small bowel that was adhered and clustered. Various bowel wall abnormalities could be present in the adhered and clustered small bowel segments. Heterogeneity in the bowel wall texture was commonly striking in the adhered small bowel segment. The lumen could be either gas-filled or liquid-filled and frequently alternated. Gas-liquid levels are frequently present in the lumen of the small bowel, indicating the presence of dynamical abnormalities. Bowel wall thickening and transmural inflammatory changes, such as mesenteric fat deposition, increased vasculature and fibrotic peritoneal thickening, were usually particularly striking in the adhered bowel segments. A segment of adhesive bowel loop with peritoneal involvement forms the so-called “abdominal cocoon”[29-32]. In this study, various abdominal cocoons, such as the “accordion sign”, “cauliflower sign” and “bottle gourd sign”, were found. An adhesive bowel loop was present in 15 patients [Figure 1 (case 4), Figure 9 (case 13), Figure 2 (case 3), Figure 3 (case 6), Figure 4 (case 9), Figure 16 (case 12), Figure 13 (case 14), Figure 5 (case 15), Figure 10 (case 11), Figure 6 (case 2), Figure 11 (case 17), Figure 7 (case 1), Figure 8 (case 7), Figure 14 (case 8), and Figure 17 (case 16)]. The high incidence of an adhesive bowel loop suggested the presence of high prevalence of chronic active bowel inflammatory damage in the small intestine in patients with SAA. In the 2 patients without an adhesive bowel loop, Figure 15 (case 10) and Figure 17 (case 5) presented with striking hypervascular mesenteric fat proliferation and a widened bowel loop (creeping fat sign), also indicating the presence of active



DOI: 10.12998/wjcc.v11.i3.576 Copyright ©The Author(s) 2023.

Figure 10 Characteristic images in case 11. A-C: Characteristic images of the ascending colon. The ascending colon was rugged with fibrotically and irregularly thickened colonic mucosa, circumferentially distributed omental thickening and paracolic fat stranding (yellow arrows), and other colonic segments were thickened and stratified with water halo sign (red arrows); D-F: Characteristic images of the ileocecal region. The ileocecal valve and the terminal ileal wall were strikingly thickened and stratified (orange arrows). Bowel wall thickening, mural stratification, heterogeneity in bowel wall texture and gas-liquid levels (purple arrows) were found in the small intestine; G-I: Stratified thickening of the large intestine. From the hepatic flexure to the sigmoid colon, the colonic wall was thickened and stratified with water halo sign (red arrows). Several inflamed diverticula was present in the colonic segments (white arrows). A segment of adhesive bowel loop was present in the middle jejunum (blue arrows), together with the peritoneal involvement forming the so-called “cauliflower sign”.

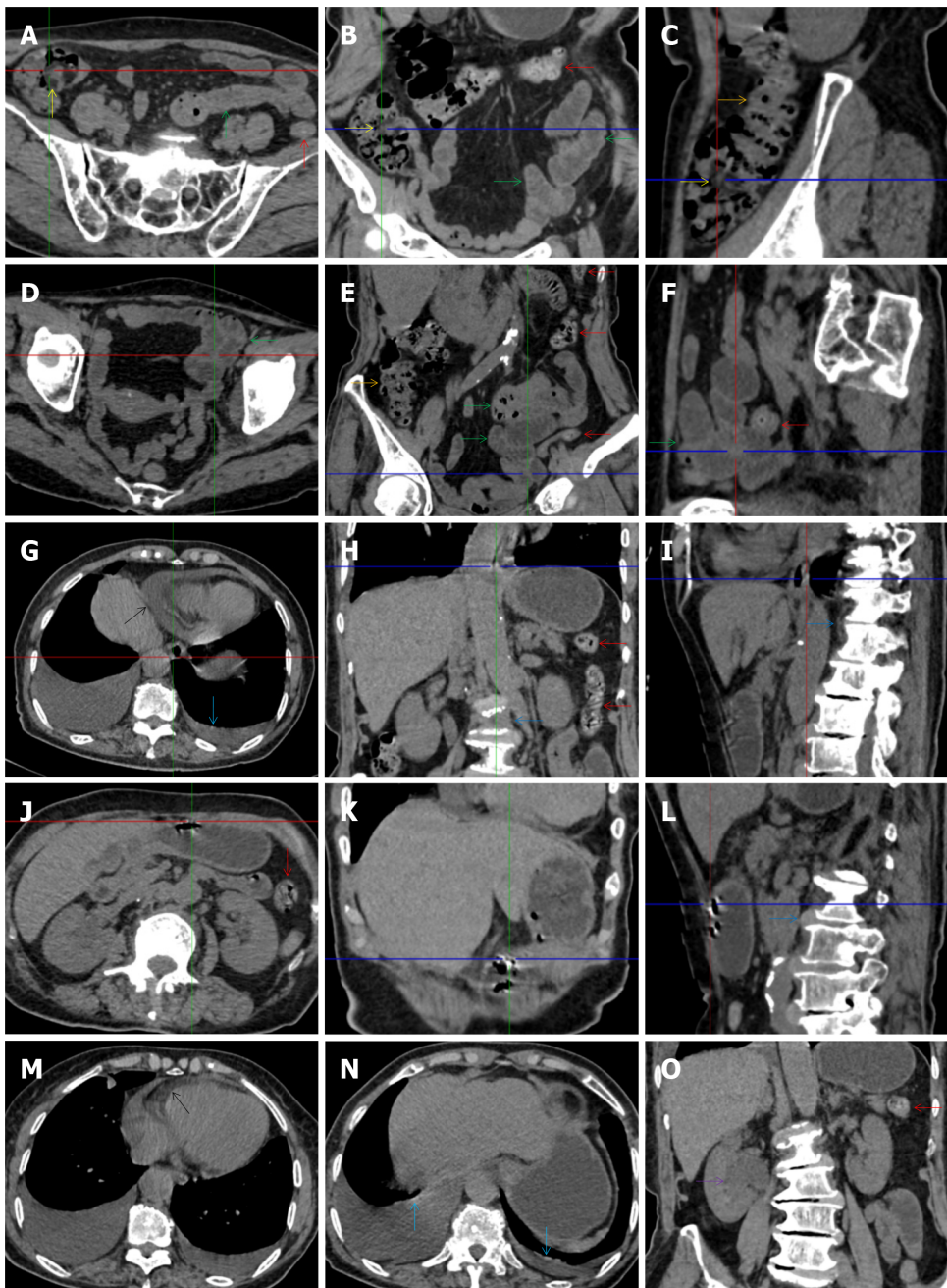
chronic inflammatory involvement of the small intestine[24-26]. Although these inflammatory lesions in the small bowel might not serve as the major factors in the regulation of hematopoietic and immune functions, they exert an important role that affects the downstream gut microbial community and thereby affects downstream intestinal barrier function[54-56].

The ileocecal region is the most common site for various infectious and inflammatory diseases[9,10,14,16]. In this study, all patients with SAA presented with inflammatory involvement of the ileocecal region. Among them, 2 patients presented with inflammatory lesions in the ileocecal region as the predominant imaging presentation. In Figure 7 (case 1), the prominent inflammatory lesion was a large omentum-encapsulated inflammatory mass centered on the homogeneously wall-thickened appendix and extending to the scrotum along the inguinal canal. In Figure 8 (case 7), the particularly prominent inflammatory lesion was a cluster of misty fat stranding wrapping the thickened and strictured distal ileum.

Concomitant extraabdominal presentations may confer useful information for a suggestive etiopathological diagnosis. In this study, pleural involvement of hypertrophic lesions was present in 4 patients [Figure 5 (case 5), Figure 11 (case 17), Figure 14 (case 8), and Figure 12 (case 16)], strongly suggestive of tuberculosis infection. However, no tuberculous lesions were present in their lungs. In addition to the pleural involvement, 1 patients [Figure 9 (case 13)] presented with peritoneal involvement of hypertrophic lesions, also suggesting the presence of tuberculosis infection.

Taken together, this radiological study demonstrated the gut involvement of various inflammatory changes in all patients with SAA. The inflammatory lesions concurrently affected the large intestine, ileocaecal region and small intestine. Although compromised intestinal integrity in the ileocecal region and large intestine exerts a major role in the development of hematological and immunological diseases [9-13], inflammatory damage and dysfunction in the upper gastrointestinal tract can affect the pathophysiologies of the downstream intestinal integrity[54-56] and thereby exert an indirect impact on hematological and immunological function. In susceptible individuals, active chronic gut inflammatory conditions may initiate and perpetuate hematological damage, and aggravated gut damages may induce flared episodes[4-8].

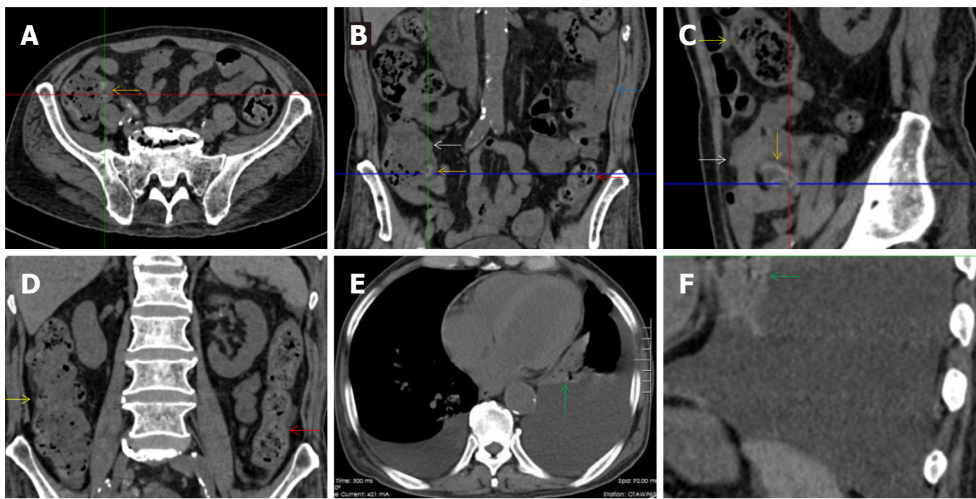
During flared episodes, the imaging features suggested the presence of chronic gut inflammatory conditions and acutely aggravated inflammatory damages. Some readily recognized imaging signs, such as bowel wall thickening with mural stratification (“water halo sign”, “fat halo sign”, intramural



DOI: 10.12998/wjcc.v11.i3.576 Copyright ©The Author(s) 2023.

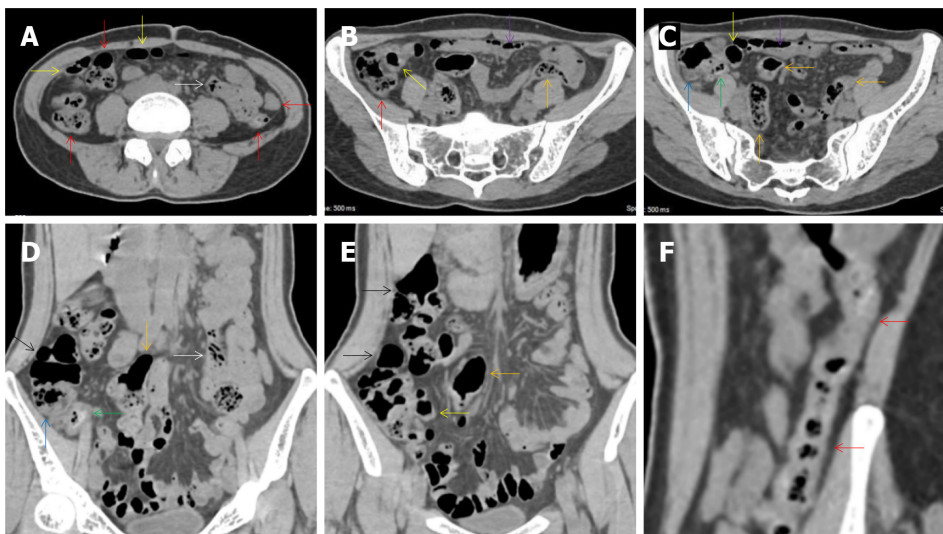
Figure 11 Characteristic images in case 17. A-C: Characteristic images of the ileocecal region and the ascending colon. Circumferentially distributed fat deposition wrapped the ileocecal valve (yellow arrows), forming the so-called “fat halo sign”. The terminal ileum was thickened, and the strictured ileocecal valve and terminal ileum led to the small intestines being liquid-filled. Heterogeneity and hypertrophic lesions of the small intestines were easily recognized. The ascending colon was rugged with paracolonic fat stranding and peritoneal thickening, and the colonic wall was thickened and stratified with edematous submucosal tissue and intramural gas (orange arrows). From the transverse to the sigmoid colon (red arrows), the colonic wall was fibrotically thickened, with multiple inflamed diverticula in this colonic segment; D-F: Characteristic images of an adhered jejunal segment. A long segment of the adhered jejunal loop was present in the left iliac fossa and pelvic cavity (green arrows). In the adhesive jejunal loop, the lumen was gas-filled in the proximal segment and liquid-filled in the distal segment. Hypervascular mesenteric fat stranding and fibrotic peritoneal thickening were present in this bowel segment, forming the so-called “abdominal cocoon”. Fibrotic wall thickening was present in the entire jejunal segment and accrescent pili were visualized in the adhesive jejunal loop and the proximal jejunum; G-I: Erosive lesions in extraintestinal organs. Erosive lesions on the background of the calcified lesions were found in the esophagus. Hypertrophic lesions and seromembranous effusion were visualized in the pericardium (black arrows) and the pleura (light blue arrows). Exudative lesions were also present in the vertebral column (blue arrows); J-L: Erosive lesions in the stomach. Erosive lesions on the background of the calcified lesions were also found in the stomach; M-O: Exudative lesions in extraintestinal organ. Hypertrophic lesions and seromembranous effusion were visualized in the pericardium (black arrows) and the pleura (light blue arrows). Exudative lesions were also present in the renal pelvis and urinary tract (a purple arrow). These radiological features led to the diagnosis of reactive tuberculosis infections in the gastrointestinal tract, urinary tract, peritoneum, vertebral column, pleura and pericardium.

gas and subserosal pneumatoses) and mesenteric fat proliferation (fat stranding and “creeping fat sign”), “balloon sign”, rugged colonic configuration and adhesive bowel loop (including various patterns of abdominal cocoon), occurred at a high incidence, which suggested that the gastrointestinal



DOI: 10.12998/wjcc.v11.i3.576 Copyright ©The Author(s) 2023.

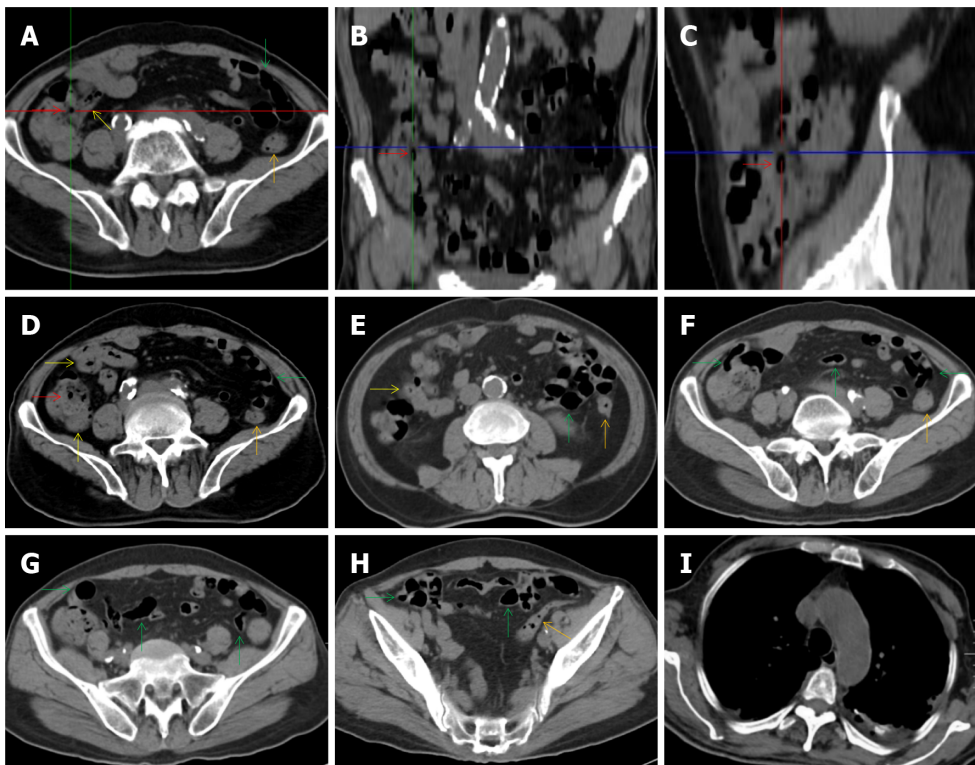
Figure 12 Characteristic images in case 16. A-C: Characteristic images of the ileocecal region and the small intestine. The ileocecal valve was fibrotic and thickened with edematous fat deposition, forming the so-called “fat halo sign” (orange arrows), and the distal ileum was adhesive with mesenteric fat stranding and peritoneal thickening (white arrow), forming the so-called “abdominal cocoon”. Intestinal adhesion with bowel wall thickening, peritoneal involvement and mesenteric fat stranding was also found in the jejunum (blue arrow). Heterogeneity in the bowel wall texture was particularly prominent in the adhesive bowel segments; D: Characteristic image of the large intestine. The ascending colon was rugged and the colonic wall was thickened and stratified, with adjacent omental thickening (yellow arrows). The descending colonic wall were significantly thickened and stratified with mucosal hyperdensity and paracolic fat stranding (red arrows); E and F: Characteristic images of the chest computed tomography (CT) scan. Chest CT revealed that the pleural effusion was predominantly in the left cavity and hypertrophic lesions involved both the left pleura and the pericardium (green arrows).



DOI: 10.12998/wjcc.v11.i3.576 Copyright ©The Author(s) 2023.

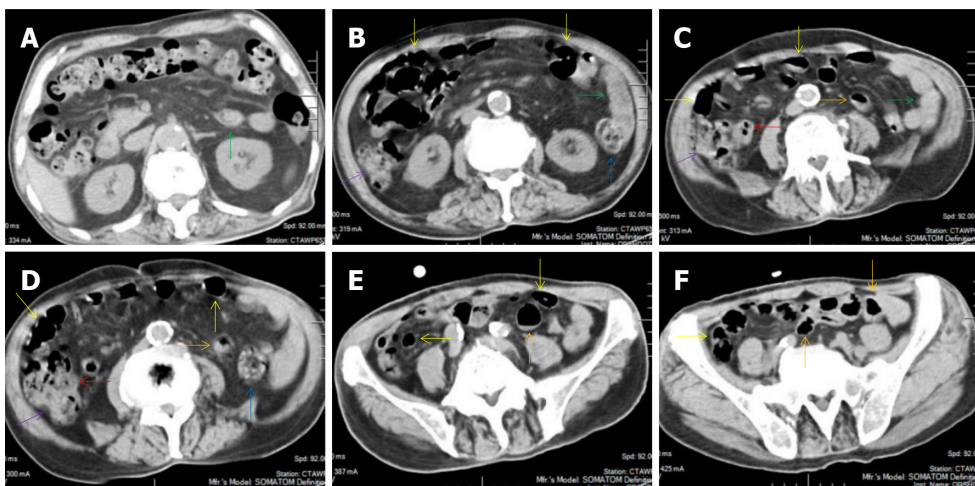
Figure 13 Characteristic images of case 14. A-C: Characteristic images of the bowel inflammatory lesions. The ileocecal valve and the ileal wall were fibrotically thickened and the ileal lumen was gas-filled (yellow arrows), with a large cluster of hypervascular perienteric fat proliferation wrapping the wall-thickened and lumen-dilated ileum. The cecum (blue arrows) and appendix (green arrows) were also fibrotically thickened and stratified, with peripheral fat stranding. Gas-liquid levels were present in the lumen of the proximal ileum and distal jejunum (purple arrows). However, the adhesive jejunal loop was liquid-filled with prominent hypervascular mesenteric fat proliferation. In a segment of the jejunum (white arrows), the bowel wall was thickened, the lumen was gas-filled and the mesenteric fat stranding was especially prominent. Thickened peritoneum was adjacent to the adhesive jejunal loop, forming the so-call “abdominal cocoon” and the enlarged mesenteric vascularity formed the so-called “comb sign”. The ascending colon was dilated with a paper-thin bowel wall (black arrows), forming the so-called “balloon sign”. From the hepatic flexure to the distal descending colon (red arrows), the bowel was thickened and stratified (water halo sign), with paracolic fat stranding and peritoneal thickening being particular prominent in the hepatic flexure. The sigmoid colon was fibrotically thickened and dilated (orange arrows); D and E: Characteristic images in coronally reconstructed images. The coronally reconstructed images better outlined the above-mentioned imaging features; F: Characteristic image of the descending colon in coronally reconstructed section. A coronally reconstructed image better outlined the thickened and stratified descending colon.

tract is common inflammatory niche responsible for the systemic inflammatory stresses in patients with SAA. Successful treatment of their gut inflammatory conditions significantly improves their hematological profile[4-6], providing convincing evidence for a role of gut inflammation in hematopoietic suppression.



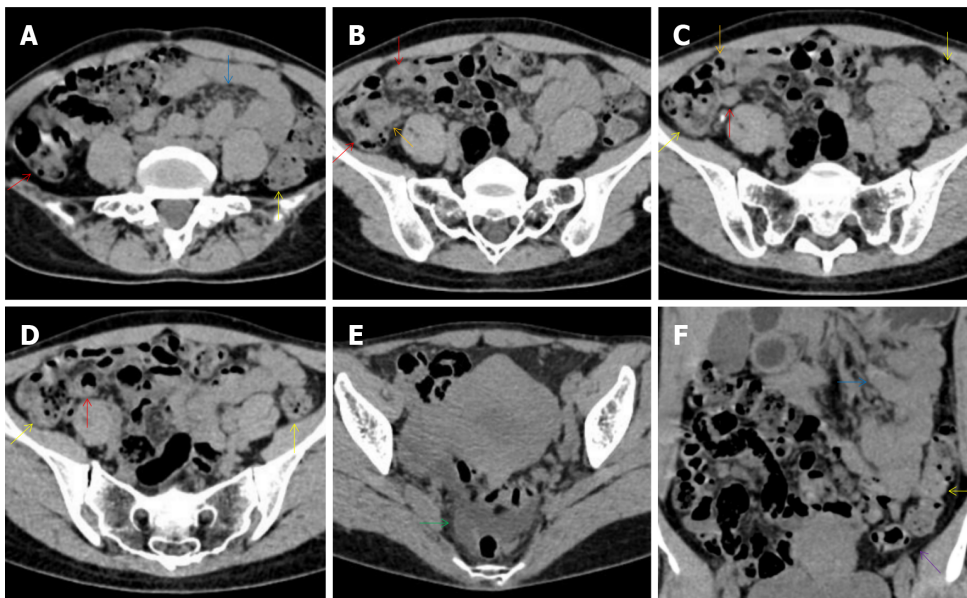
DOI: 10.12998/wjcc.v11.i3.576 Copyright ©The Author(s) 2023.

Figure 14 Characteristic images in case 8. A-C: Characteristic images of the ileocecal region and the small intestine. The ileocecal valve (red arrows) was thickened, strictured and stratified. The distal ileum (yellow arrows) were significantly thickened with intramural gas and wrapped by prominent mesenteric fat stranding, which suggested the presence of aggravated inflammatory damage in the distal ileum and ileocecal region; D-H: Characteristic images of the small intestine. In the ileocecal region, the ileum adhered to the cecum, and the cecum was thickened and stratified. In other colonic segments (orange arrows), the bowel wall was also thickened and stratified, and the lumen was dilated in some segments and collapsed in other segments. From the jejunum to the proximal ileum (green arrows), the wall was fibrotic and thickened and the lumen was gas-filled. Several segments of adhesive bowel loop were present in the small bowel. Noticeably, panabdominal silt-like hypervascular fat deposition wrapped the adhesive and widened small bowel loop (creeping fat sign), which suggested the presence of chronic transmural inflammatory damage and a diagnosis of Crohn's disease; I: Characteristic image of the chest computed tomography (CT) scan. Chest CT showed exudative lesions in the left pleura in the context of calcified lesions, indicating the reactivation of an old tuberculosis infection.



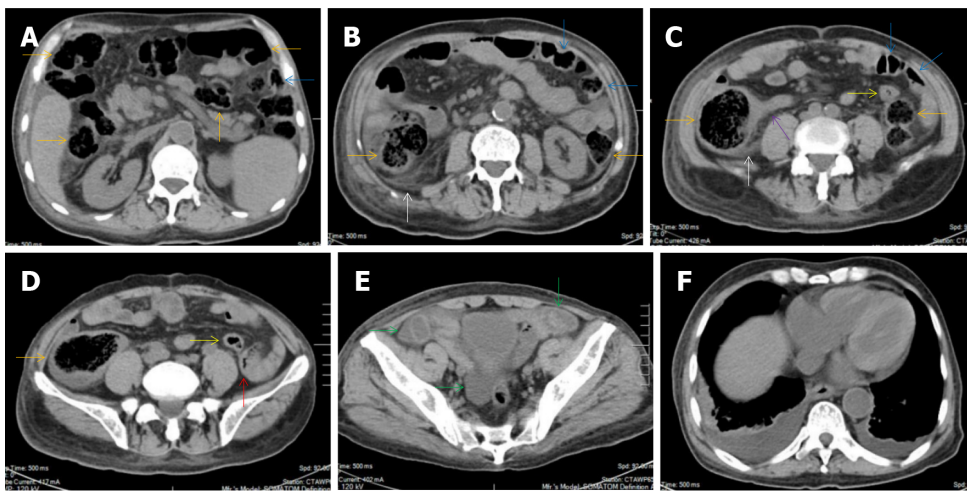
DOI: 10.12998/wjcc.v11.i3.576 Copyright ©The Author(s) 2023.

Figure 15 Characteristic images of case 10. A and B: Characteristic images of the fat deposition. The most noticeable radiological finding was the panabdominal silt-like hypervascular fat deposition, leading to the widening of the bowel loop of the jejunum and the proximal ileum, forming the so-called "creeping fat sign". The ileum was fibritically thickened and dilated, and the duodenum and the proximal jejunum were liquid-filled (green arrows); C and D: Characteristic images of the ileocecal region. The ileocecal valve and the terminal ileum were significantly thickened, stratified and strictured (red arrows), and proximal to the thickened terminal ileum, the ileal lumen was dilated and gas-filled and the mucosa was hyperdense (yellow arrows). The ascending colonic wall was also thickened (purple arrows). In a short segment of the descending colon (blue arrows), accrescent villi were especially prominent; E and F: Characteristic images of the small intestine. The proximal ileum and the distal jejunum (orange arrows) were thickened and gas-filled.



DOI: 10.12998/wjcc.v11.i3.576 Copyright ©The Author(s) 2023.

Figure 16 Characteristic images of case 12. A-D: Characteristic images of the bowel inflammatory lesions. The ileocecal valve and the terminal ileal wall (red arrows) were thickened, stratified and strictured. Proximal to the strictured terminal ileum, the ileal lumen was dilated and gas-filled, and the mucosa was hyperdense. A large cluster of hypervascular mesenteric fat proliferation wrapped the dilated and gas-filled ileum. The jejunum was liquid-filled and the jejunal loop was adhesive. A cluster of hypervascular fat stranding wrapped a short segment of the jejunum (blue arrows), suggesting that the transmural inflammation was more serious in this jejunal segment. The colonic wall was also thickened and stratified, with intramural gas and subserosal pneumatosis (yellow arrows); E: Characteristic image of the pelvic liquid collection. Mild liquid collection was present in the pelvic cavity (a green arrow), together with the thickened peritoneum (a purple arrow) suggesting the presence of peritoneal involvement; F: Characteristic image in coronally reconstructed section. A coronally reconstructed image better outlined the above-mentioned imaging features.



DOI: 10.12998/wjcc.v11.i3.576 Copyright ©The Author(s) 2023.

Figure 17 Characteristic images of case 5. A-D: Characteristic images of the bowel inflammatory lesions. From the cecum to the descending colon, the lumen was dilated, the mucosa was hyperdense and the wall was thickened and stratified in some segments (orange arrows), with striking mesenteric fat stranding. There was a hypertrophic lesion (a red arrow) in the terminal descending colon. The mucosa of the proximal sigmoid colon was hyperdense and the lumen was gas-filled (blue arrows), following which was a short segment of strictured sigmoid colon (yellow arrows). The ileocecal valve and the terminal ileum were thickened and strictured but without mural stratification (a purple arrow), proximal to which the small intestine was liquid-filled. In the ileocecal region, the colonic wall was thickened with smudgy peritoneal thickening (white arrows); E: Characteristic image of the pelvic liquid collection. Mild ascites was present in both the right and left iliac fossa (green arrows), together with a thickened peritoneum suggesting the presence of peritoneal involvement; F: Characteristic image of the chest computed tomography (CT) scan. Chest CT showed the presence of pleural effusion in the bilateral cavities and bilateral pleural hypertrophic thickening. Enlarged blood vessels extended to the hypertrophic lesions.

Although not able to provide an etiopathological diagnosis, abdominal CT can provide useful information for exploring gut inflammatory conditions and guiding further work-ups. In this study, a suggestive diagnosis of Crohn's disease was made in 5 patients, ulcerative colitis in 1 patient, chronic periappendiceal abscess in 1 patient, and tuberculosis infection in 5 patients[57-59]. Although the

presence of abdominal cocoons has been reported to have a high probability of tuberculosis infection[31, 32] and there was a high incidence of abdominal cocoons present in this study, it was difficult to make a presumptive diagnosis of tuberculosis infection in patients with abdominal cocoons other than the abovementioned 5 patients.

This study had several limitations. First, although CT has some advantages in the detection of the site, extent, degree and peripheral changes of gut inflammatory damage, the exact pathogenic factors cannot be identified, and arriving at an etiopathological diagnosis frequently requires other laboratory tests. This study lacked the endoscopic, pathological and other definitive diagnostic examinations largely due to the contraindication of invasive operative procedures resulting from the very low platelet count and the platelet transfusion refractoriness of these patients. Second, the number of studied patients was quite small, leading to the incidence of each imaging sign being less representative of the actual incidence. Third, the treatment responses by suggested radiological diagnosis were not summarized.

CONCLUSION

All patients with SAA during inflammatory episodes demonstrated gut involvement of both active chronic inflammatory conditions and acute inflammatory damage, providing further evidence to demonstrate the role of GIDs in the pathogenesis of immune-mediated hematopoietic failure. Although arriving at an etiopathological diagnosis frequently requires other laboratory tests, abdominal CT imaging can provide highly useful information for the exploration of gut inflammatory damage and is very helpful for the suggestion of an effective treatment modality. In patients with aggravated cytopenia and clinical presentations suggestive of the presence of inflammatory responses, inflammatory diseases in the gastrointestinal tract should be considered, abdominal CT should be performed, and imaging signs that suggest the presence of gut inflammatory lesions should be carefully identified.

ARTICLE HIGHLIGHTS

Research background

The gastrointestinal tract hosts the body's most enriched lymphoid tissues and microbial community and therefore can provide sufficient activated immune cells and continuous intestine-derived antigens to influence the host hematopoietic and immune functions. The gastrointestinal tract is the most common site for infectious and inflammatory diseases. Morphological changes on computed tomography (CT) images can provide useful information that reflects the distribution, extent, and severity of the bowel inflammation and even suggests a pathogenic diagnosis.

Research motivation

Initiation and perpetuation of aplastic anemia (AA) pathogenesis has been found to be associated with gut inflammatory disorders (GIDs). GIDs have a powerful impact on hematopoietic and immune functions. Treatment of GIDs can improve hematological profile and immunological derangement.

Research objectives

To explore CT imaging presentations of gut inflammatory damage in adult patients with severe AA (SAA) and to provoke awareness of GIDs in the pathogenesis of hematological and autoimmune disorders.

Research methods

We retrospectively evaluated the abdominal CT imaging presentations of 17 hospitalized adult patients with SAA in search of the inflammatory niche when they presented with systemic inflammatory stress and exacerbated hematopoietic function.

Research results

All eligible patients with SAA had CT imaging abnormalities that suggested the presence of an impaired intestinal barrier and increased epithelial permeability. The inflammatory damages were concurrently present in the small intestine, the ileocecal region and the large intestines.

Research conclusions

All patients with SAA had CT imaging patterns that suggested the presence of active chronic inflammatory conditions and aggravated inflammatory damage during flared inflammatory episodes. In patients with aggravated cytopenia and clinical presentations suggestive of the presence of inflammatory responses, inflammatory diseases in the gastrointestinal tract should be considered, abdominal CT should be performed, and imaging signs that suggest the presence of gut inflammatory lesions

should be carefully identified.

Research perspectives

Abdominal CT imaging presentations in association with hematopoietic failure and autoimmune diseases warrant extensive investigations.

FOOTNOTES

Author contributions: Zhao XC and Xiao SX developed the idea; Zhao XC and Xue CJ organized the study; Zhao XC, Xue CJ, Song H, Gao BH, Han FS, and Xiao SX reviewed and consulted the CT images; Zhao XC drafted the manuscript; Xiao SX revised and approved the final manuscript; all authors have read and approved the final version of the manuscript.

Supported by the Specialized Scientific Research Fund Projects of the Medical Group of Qingdao University, No. YLJT20201002.

Institutional review board statement: The study was reviewed and approved by the Central Hospital of Qingdao West Coast New Area Institutional Review Board (Approval No. 2022-10-08).

Informed consent statement: The requirement of written informed consent was waived by The Ethics Committee of The Central Hospital of Qingdao West Coast New Area since this was a retrospective study and no information linked to the patients' identity was revealed in the manuscript.

Conflict-of-interest statement: The authors have no conflicts of interest to declare that are relevant to the content of this article.

Data sharing statement: No additional data are available.

Open-Access: This article is an open-access article that was selected by an in-house editor and fully peer-reviewed by external reviewers. It is distributed in accordance with the Creative Commons Attribution NonCommercial (CC BY-NC 4.0) license, which permits others to distribute, remix, adapt, build upon this work non-commercially, and license their derivative works on different terms, provided the original work is properly cited and the use is non-commercial. See: <https://creativecommons.org/licenses/by-nc/4.0/>

Country/Territory of origin: China

ORCID number: Xi-Chen Zhao 0000-0002-3304-2851; Cheng-Jiang Xue 0000-0002-8763-9901; Hui Song 0000-0002-6347-4006; Bin-Han Gao 0000-0002-7916-546X; Fu-Shen Han 0000-0002-5630-5730; Shu-Xin Xiao 0000-0003-0821-6968.

S-Editor: Chen YL

L-Editor: A

P-Editor: Zhao S

REFERENCES

- Giudice V, Sellari C. Aplastic anemia: Pathophysiology. *Semin Hematol* 2022; **59**: 13-20 [PMID: 35491054 DOI: 10.1053/j.seminhematol.2021.12.002]
- Patel BA, Giudice V, Young NS. Immunologic effects on the haematopoietic stem cell in marrow failure. *Best Pract Res Clin Haematol* 2021; **34**: 101276 [PMID: 34404528 DOI: 10.1016/j.beha.2021.101276]
- Killick SB, Bown N, Cavenagh J, Dokal I, Foukaneli T, Hill A, Hillmen P, Ireland R, Kulasekararaj A, Mufti G, Snowden JA, Samarasinghe S, Wood A, Marsh JC; British Society for Standards in Haematology. Guidelines for the diagnosis and management of adult aplastic anaemia. *Br J Haematol* 2016; **172**: 187-207 [PMID: 26568159 DOI: 10.1111/bjh.13853]
- Zhao XC, Zhao L, Sun XY, Xu ZS, Ju B, Meng FJ, Zhao HG. Excellent response of severe aplastic anemia to treatment of gut inflammation: A case report and review of the literature. *World J Clin Cases* 2020; **8**: 425-435 [PMID: 32047795 DOI: 10.12998/wjcc.v8.i2.425]
- Salmeron G, Patey N, de Latour RP, Raffoux E, Gluckman E, Brousse N, Socié G, Robin M. Coeliac disease and aplastic anaemia: a specific entity? *Br J Haematol* 2009; **146**: 122-124 [PMID: 19438483 DOI: 10.1111/j.1365-2141.2009.07719.x]
- Tokar B, Aydođdu S, Pařaođlu O, Ilhan H, Kasapođlu E. Neutropenic enterocolitis: is it possible to break vicious circle between neutropenia and the bowel wall inflammation by surgery? *Int J Colorectal Dis* 2003; **18**: 455-458 [PMID: 12750931 DOI: 10.1007/s00384-003-0502-3]
- Espinoza JL, Elbadry MI, Nakao S. An altered gut microbiota may trigger autoimmune-mediated acquired bone marrow failure syndromes. *Clin Immunol* 2016; **171**: 62-64 [PMID: 27506961 DOI: 10.1016/j.clim.2016.08.008]
- Zhao XC, Sun XY, Zhao L, Meng FJ. Gut inflammation in the pathogenesis of acquired aplastic anemia. *Chin Med J (Engl)* 2020; **133**: 1878-1881 [PMID: 32568881 DOI: 10.1097/CM9.0000000000000772]

- 9 **Shen L.** Functional morphology of the gastrointestinal tract. *Curr Top Microbiol Immunol* 2009; **337**: 1-35 [PMID: 19812978 DOI: 10.1007/978-3-642-01846-6_1]
- 10 **Guven-Maiorov E, Tsai CJ, Nussinov R.** Structural host-microbiota interaction networks. *PLoS Comput Biol* 2017; **13**: e1005579 [PMID: 29023448 DOI: 10.1371/journal.pcbi.1005579]
- 11 **Fasano A.** All disease begins in the (leaky) gut: role of zonulin-mediated gut permeability in the pathogenesis of some chronic inflammatory diseases. *F1000Res* 2020; **9** [PMID: 32051759 DOI: 10.12688/f1000research.20510.1]
- 12 **Mu Q, Kirby J, Reilly CM, Luo XM.** Leaky Gut As a Danger Signal for Autoimmune Diseases. *Front Immunol* 2017; **8**: 598 [PMID: 28588585 DOI: 10.3389/fimmu.2017.00598]
- 13 **Vogelzang A, Guerrini MM, Minato N, Fagarasan S.** Microbiota - an amplifier of autoimmunity. *Curr Opin Immunol* 2018; **55**: 15-21 [PMID: 30248521 DOI: 10.1016/j.coi.2018.09.003]
- 14 **Duffin C, Mirpour S, Catanzano T, Moore C.** Radiologic Imaging of Bowel Infections. *Semin Ultrasound CT MR* 2020; **41**: 33-45 [PMID: 31964493 DOI: 10.1053/j.sult.2019.10.004]
- 15 **Yu SJ, Heo JH, Choi EJ, Kim JH, Lee HS, Kim SY, Lim JH.** Role of multidetector computed tomography in patients with acute infectious colitis. *World J Clin Cases* 2022; **10**: 3686-3697 [PMID: 35647171 DOI: 10.12998/wjcc.v10.i12.3686]
- 16 **Hines JJ Jr, Mikhitarian MA, Patel R, Choy A.** Spectrum and Relevance of Incidental Bowel Findings on Computed Tomography. *Radiol Clin North Am* 2021; **59**: 647-660 [PMID: 34053611 DOI: 10.1016/j.rcl.2021.03.012]
- 17 **Fernandes T, Oliveira MI, Castro R, Araújo B, Viamonte B, Cunha R.** Bowel wall thickening at CT: simplifying the diagnosis. *Insights Imaging* 2014; **5**: 195-208 [PMID: 24407923 DOI: 10.1007/s13244-013-0308-y]
- 18 **Mills A, Mellnick VM, Itani M.** Imaging of Bowel Wall Thickening in the Hospitalized Patient. *Radiol Clin North Am* 2020; **58**: 1-17 [PMID: 31731894 DOI: 10.1016/j.rcl.2019.08.006]
- 19 **Agarwala R, Singh AK, Shah J, Mandavdhare HS, Sharma V.** Ileocecal thickening: Clinical approach to a common problem. *JGH Open* 2019; **3**: 456-463 [PMID: 31832544 DOI: 10.1002/jgh3.12186]
- 20 **Marín-Díez E, Crespo Del Pozo J.** Diagnostic approach to small-bowel wall thickening: beyond Crohn's disease and cancer. *Radiologia (Engl Ed)* 2021 [PMID: 33546910 DOI: 10.1016/j.rx.2020.11.010]
- 21 **Wang X, Yuan M, Mi H, Suo S, Eteer K, Li S, Lu Q, Xu J, Hu J.** The feasibility of differentiating colorectal cancer from normal and inflammatory thickening colon wall using CT texture analysis. *Sci Rep* 2020; **10**: 6346 [PMID: 32286352 DOI: 10.1038/s41598-020-62973-1]
- 22 **Thornton E, Mendiratta-Lala M, Siewert B, Eisenberg RL.** Patterns of fat stranding. *AJR Am J Roentgenol* 2011; **197**: W1-14 [PMID: 21700969 DOI: 10.2214/AJR.10.4375]
- 23 **Pereira JM, Sirlin CB, Pinto PS, Jeffrey RB, Stella DL, Casola G.** Disproportionate fat stranding: a helpful CT sign in patients with acute abdominal pain. *Radiographics* 2004; **24**: 703-715 [PMID: 15143223 DOI: 10.1148/rg.243035084]
- 24 **Xiong S, Tan J, Wang Y, He J, Hu F, Wu X, Liu Z, Lin S, Li X, Chen Z, Mao R.** Fibrosis in fat: From other diseases to Crohn's disease. *Front Immunol* 2022; **13**: 935275 [PMID: 36091035 DOI: 10.3389/fimmu.2022.935275]
- 25 **Suau R, Pardina E, Domènech E, Lorén V, Manyé J.** The Complex Relationship Between Microbiota, Immune Response and Creeping Fat in Crohn's Disease. *J Crohns Colitis* 2022; **16**: 472-489 [PMID: 34528668 DOI: 10.1093/ecco-jcc/jjab159]
- 26 **Ha CWY, Martin A, Sepich-Poore GD, Shi B, Wang Y, Gouin K, Humphrey G, Sanders K, Ratnayake Y, Chan KSL, Hendrick G, Caldera JR, Arias C, Moskowitz JE, Ho Sui SJ, Yang S, Underhill D, Brady MJ, Knott S, Kaihara K, Steinbaugh MJ, Li H, McGovern DPB, Knight R, Fleshner P, Devkota S.** Translocation of Viable Gut Microbiota to Mesenteric Adipose Drives Formation of Creeping Fat in Humans. *Cell* 2020; **183**: 666-683.e17 [PMID: 32991841 DOI: 10.1016/j.cell.2020.09.009]
- 27 **Knox C, Almeida J.** The Comb Sign. *Clin Gastroenterol Hepatol* 2021; **19**: A29-A30 [PMID: 32634621 DOI: 10.1016/j.cgh.2020.06.054]
- 28 **Ueda Y, Yanagi H.** The comb sign in a patient with Crohn's disease. *J Gen Fam Med* 2022; **23**: 120-121 [PMID: 35261863 DOI: 10.1002/jgf2.499]
- 29 **Basara Akin I, Altay C, Celik A, Secil M.** Computed Tomography Features of Encapsulating Peritoneal Sclerosis. *Can Assoc Radiol J* 2019; **70**: 233-238 [PMID: 30922787 DOI: 10.1016/j.carj.2018.11.005]
- 30 **Ethiraj D, Indiran V.** Abdominal Cocoon: "Cauliflower Sign" on Contrast-Enhanced Computed Tomography Scan. *GE Port J Gastroenterol* 2020; **28**: 76-77 [PMID: 33564710 DOI: 10.1159/000507636]
- 31 **Gorsi U, Gupta P, Mandavdhare HS, Singh H, Dutta U, Sharma V.** The use of computed tomography in the diagnosis of abdominal cocoon. *Clin Imaging* 2018; **50**: 171-174 [PMID: 29602067 DOI: 10.1016/j.clinimag.2018.03.014]
- 32 **Sharma V, Singh H, Mandavdhare HS.** Tubercular Abdominal Cocoon: Systematic Review of an Uncommon Form of Tuberculosis. *Surg Infect (Larchmt)* 2017; **18**: 736-741 [PMID: 28759335 DOI: 10.1089/sur.2017.110]
- 33 **Ling J, Dyer RB.** The "hot air balloon" sign. *Abdom Radiol (NY)* 2019; **44**: 2663-2664 [PMID: 30850891 DOI: 10.1007/s00261-019-01972-x]
- 34 **LoVerde ZJ, Dyer RB.** "Lâcher de ballons" or "release of balloons" sign. *Abdom Radiol (NY)* 2018; **43**: 2208-2209 [PMID: 29260277 DOI: 10.1007/s00261-017-1428-5]
- 35 **Rodríguez-Otero Luppi C, Rodríguez Blanco M, Bollo Rodríguez J, Méndez A, Merlo Más J.** Laparoscopic resection of a giant colonic diverticulum - the 'lifting balloon' sign - a video vignette. *Colorectal Dis* 2019; **21**: 1096-1098 [PMID: 31120633 DOI: 10.1111/codi.14716]
- 36 **Heylen CE, Pringot J, Van Belle K.** The Lifting Balloon: Sign of a Giant Colonic Diverticulum. *J Belg Soc Radiol* 2017; **101**: 26 [PMID: 30039018 DOI: 10.5334/jbr-btr.1363]
- 37 **Wang J, Erlacher M, Fernandez-Orth J.** The role of inflammation in hematopoiesis and bone marrow failure: What can we learn from mouse models? *Front Immunol* 2022; **13**: 951937 [PMID: 36032161 DOI: 10.3389/fimmu.2022.951937]
- 38 **Espinoza JL, Kotecha R, Nakao S.** Microbe-Induced Inflammatory Signals Triggering Acquired Bone Marrow Failure Syndromes. *Front Immunol* 2017; **8**: 186 [PMID: 28286502 DOI: 10.3389/fimmu.2017.00186]
- 39 **Boiko JR, Borghesi L.** Hematopoiesis sculpted by pathogens: Toll-like receptors and inflammatory mediators directly activate stem cells. *Cytokine* 2012; **57**: 1-8 [PMID: 22079335 DOI: 10.1016/j.cyto.2011.10.005]

- 40 **Chiba Y**, Mizoguchi I, Hasegawa H, Ohashi M, Orii N, Nagai T, Sugahara M, Miyamoto Y, Xu M, Owaki T, Yoshimoto T. Regulation of myelopoiesis by proinflammatory cytokines in infectious diseases. *Cell Mol Life Sci* 2018; **75**: 1363-1376 [PMID: 29218601 DOI: 10.1007/s00018-017-2724-5]
- 41 **Esplin BL**, Shimazu T, Welner RS, Garrett KP, Nie L, Zhang Q, Humphrey MB, Yang Q, Borghesi LA, Kincaid PW. Chronic exposure to a TLR ligand injures hematopoietic stem cells. *J Immunol* 2011; **186**: 5367-5375 [PMID: 21441445 DOI: 10.4049/jimmunol.1003438]
- 42 **MacNamara KC**, Racine R, Chatterjee M, Borjesson D, Winslow GM. Diminished hematopoietic activity associated with alterations in innate and adaptive immunity in a mouse model of human monocytic ehrlichiosis. *Infect Immun* 2009; **77**: 4061-4069 [PMID: 19451243 DOI: 10.1128/IAI.01550-08]
- 43 **Rodriguez S**, Chora A, Goumnerov B, Mumaw C, Goebel WS, Fernandez L, Baydoun H, HogenEsch H, Dombkowski DM, Karlewicz CA, Rice S, Rahme LG, Carlesso N. Dysfunctional expansion of hematopoietic stem cells and block of myeloid differentiation in lethal sepsis. *Blood* 2009; **114**: 4064-4076 [PMID: 19696201 DOI: 10.1182/blood-2009-04-214916]
- 44 **Maratheftis CI**, Andreacos E, Moutsopoulos HM, Voulgarelis M. Toll-like receptor-4 is up-regulated in hematopoietic progenitor cells and contributes to increased apoptosis in myelodysplastic syndromes. *Clin Cancer Res* 2007; **13**: 1154-1160 [PMID: 17317824 DOI: 10.1158/1078-0432.CCR-06-2108]
- 45 **Giudice V**, Feng X, Lin Z, Hu W, Zhang F, Qiao W, Ibanez MDPF, Rios O, Young NS. Deep sequencing and flow cytometric characterization of expanded effector memory CD8(+)/CD57(+) T cells frequently reveals T-cell receptor V β oligoclonality and CDR3 homology in acquired aplastic anemia. *Haematologica* 2018; **103**: 759-769 [PMID: 29419434 DOI: 10.3324/haematol.2017.176701]
- 46 **Chaturvedi CP**, Tripathy NK, Minocha E, Sharma A, Rahman K, Nityanand S. Altered Expression of Hematopoiesis Regulatory Molecules in Lipopolysaccharide-Induced Bone Marrow Mesenchymal Stem Cells of Patients with Aplastic Anemia. *Stem Cells Int* 2018; **2018**: 6901761 [PMID: 30416525 DOI: 10.1155/2018/6901761]
- 47 **Adolph TE**, Zhang J. Diet fuelling inflammatory bowel diseases: preclinical and clinical concepts. *Gut* 2022; **71**: 2574-2586 [PMID: 36113981 DOI: 10.1136/gutjnl-2021-326575]
- 48 **Sugihara K**, Kamada N. Diet-Microbiota Interactions in Inflammatory Bowel Disease. *Nutrients* 2021; **13** [PMID: 34062869 DOI: 10.3390/nu13051533]
- 49 **Zhang P**. Influence of Foods and Nutrition on the Gut Microbiome and Implications for Intestinal Health. *Int J Mol Sci* 2022; **23** [PMID: 36076980 DOI: 10.3390/ijms23179588]
- 50 **Mamieva Z**, Poluektova E, Svistushkin V, Sobolev V, Shifrin O, Guarner F, Ivashkin V. Antibiotics, gut microbiota, and irritable bowel syndrome: What are the relations? *World J Gastroenterol* 2022; **28**: 1204-1219 [PMID: 35431513 DOI: 10.3748/wjg.v28.i12.1204]
- 51 **Gobbo MM**, Bomfim MB, Alves WY, Oliveira KC, Corsetti PP, de Almeida LA. Antibiotic-induced gut dysbiosis and autoimmune disease: A systematic review of preclinical studies. *Autoimmun Rev* 2022; **21**: 103140 [PMID: 35830954 DOI: 10.1016/j.autrev.2022.103140]
- 52 **Black J**, Sweeney L, Yuan Y, Singh H, Norton C, Czuber-Dochan W. Systematic review: the role of psychological stress in inflammatory bowel disease. *Aliment Pharmacol Ther* 2022; **56**: 1235-1249 [PMID: 36082403 DOI: 10.1111/apt.17202]
- 53 **Bonaz B**. Anti-inflammatory effects of vagal nerve stimulation with a special attention to intestinal barrier dysfunction. *Neurogastroenterol Motil* 2022; **34**: e14456 [PMID: 36097404 DOI: 10.1111/nmo.14456]
- 54 **Fakharian F**, Asgari B, Nabavi-Rad A, Sadeghi A, Soleimani N, Yadegar A, Zali MR. The interplay between Helicobacter pylori and the gut microbiota: An emerging driver influencing the immune system homeostasis and gastric carcinogenesis. *Front Cell Infect Microbiol* 2022; **12**: 953718 [PMID: 36046747 DOI: 10.3389/fcimb.2022.953718]
- 55 **Peng W**, Zhao X, Li X. Helicobacter bilis Contributes to the Occurrence of Inflammatory Bowel Disease by Inducing Host Immune Disorders. *Biomed Res Int* 2022; **2022**: 1837850 [PMID: 35983246 DOI: 10.1155/2022/1837850]
- 56 **Qi Y**, Zang SQ, Wei J, Yu HC, Yang Z, Wu HM, Kang Y, Tao H, Yang MF, Jin L, Zen K, Wang FY. High-throughput sequencing provides insights into oral microbiota dysbiosis in association with inflammatory bowel disease. *Genomics* 2021; **113**: 664-676 [PMID: 33010388 DOI: 10.1016/j.ygeno.2020.09.063]
- 57 **Eraksoy H**. Gastrointestinal and Abdominal Tuberculosis. *Gastroenterol Clin North Am* 2021; **50**: 341-360 [PMID: 34024445 DOI: 10.1016/j.gtc.2021.02.004]
- 58 **Gupta P**, Kumar S, Sharma V, Mandavdhare H, Dhaka N, Sinha SK, Dutta U, Kochhar R. Common and uncommon imaging features of abdominal tuberculosis. *J Med Imaging Radiat Oncol* 2019; **63**: 329-339 [PMID: 30932343 DOI: 10.1111/1754-9485.12874]
- 59 **Deshpande SS**, Joshi AR, Deshpande SS, Phajlani SA. Computed tomographic features of abdominal tuberculosis: unmask the impersonator! *Abdom Radiol (NY)* 2019; **44**: 11-21 [PMID: 30027495 DOI: 10.1007/s00261-018-1700-3]



Published by **Baishideng Publishing Group Inc**
7041 Koll Center Parkway, Suite 160, Pleasanton, CA 94566, USA
Telephone: +1-925-3991568
E-mail: bpgoffice@wjgnet.com
Help Desk: <https://www.f6publishing.com/helpdesk>
<https://www.wjgnet.com>

